Decoding Delay and Outage Performance Analysis of Full-Duplex Decode-Forward Relaying: Backward or Sliding Window Decoding

Ahmad Abu Al Haija, *Member, IEEE* and Chintha Tellambura, *Fellow, IEEE*

***Abstract*—High reliability and low latency are critical performance targets in fifth generation cellular networks. How does a full-duplex decode-forward relay fare in this context? To answer this question, we analyze the outage and (average) decoding-delay for both joint and sequential sliding window decoding. For comparison, we also analyze decoding delay of backward decoding and consider its existing outage analysis. In our analysis, We consider a block fading channel with full channel state information (CSI) availability at receivers and with limited CSI at transmitters; outage events at both relay and destination and channel variation over different blocks in sliding window decoding. Moreover, by analyzing the asymptotic performance at high SNR, we prove that both joint and sequential decoding achieve a full diversity order of two and derive the coding gain gaps between backward decoding, joint and sequential sliding window decoding. To see the benefits of full-duplex relaying, we also include the performance of half-duplex schemes and conclude that the preferred scheme depends on the rate, outage and delay requirements for a specific service.**

***Index terms*—Decode-forward relaying, backward and sliding window decoding, decoding delay, outage and diversity analysis.**

I. Introduction

Because wireless relays improve the throughput, reliability and coverage area of modern and fifth generation (5G) cellular networks, they are utilized in LTE-A release 10 [1], wireless backhaul and device-to-device (D2D) communication [2], [3]. As in Fig. 1, a relay node can be a small-cell base station connecting a user equipment (UE) to a macro-cell base station. The performance of a relaying scheme is measured by decoding delay, achievable rate, and outage, which have been analyzed extensively for half-duplex (HD) relays [4]–[9]. However, full-duplex (FD) wireless relays may potentially double the spectral efficiency [10], and hence are receiving significant research interest. They are included in 5G wireless applications such as machine-to-machine communications that require high reliability and low latency [3].

Because FD radio nodes can simultaneously transmit and receive on the same frequency, the fundamental performance limit is the signal leakage from the output of the transceiver to the input, the self-interference, which can cause significant performance degradation. This may be mitigated by millimeter waves [2], passive suppression, analog and digital cancellations [11]–[14]. Nevertheless, residual self-interference, which is seen as additive noise by the receiver [15], may be modeled by increasing the noise power received at the relay [6].

Manuscript received January 26, 2016; revised June 17, 2016; accepted August 18, 2016. This work was supported in part by grants from the Natural Science and Engineering Research Council of Canada (NSERC). This work was presented at the IEEE Global Communications Conference 2016. The associate editor coordinating the review of this paper and approving it for publication was M. Direnzo.

The authors are with the Department of Electrical and Computer Engineering, University of Alberta, Edmonton, AB T6G 1H9, Canada (e-mail: abualhai@ualberta.edu; ct4@ualberta.edu).

Color versions of one or more of the figures in this paper are available online at http://ieeexplore.ieee.org.

Digital Object Identifier 10.1109/TCOMM.2016.2603981

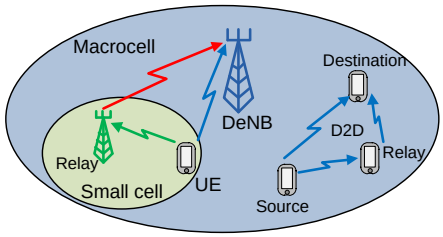

Fig. 1. Relay channel Applications in 5G networks.

Thus, these hardware and signal processing developments strongly suggest the feasibility and viability of FD radio, which is currently being trialed for cellular networks. Therefore, characterizing the performance of FD relays is beneficial for both academic and industrial researchers. The main performance measures we consider are the outage probability and decoding delay. In this paper, we define the decoding delay as the average number of transmissions blocks the destination waits before decoding the information. Hence, from now on, *decoding delay refers to block decoding delay*. We focus on FD relays with a decode-forward (DF) strategy. Thus, the relay decodes using sliding window decoding (SWD) or backward decoding (BD). In each transmission block, depending on links fading conditions, the transmission scheme switches between the direct transmission (DT) mode (i.e., relay is not transmitting) and the DF relaying mode.

A. Background and Motivation

The outage of the BD case has been analyzed for coherent [7], [16], and independent and coherent DF relaying [6]. In BD, the destination (e.g., base station in Fig. 1) initializes decoding from the last transmission block which leads to a long decoding delay. However, low latency ($\leq$ 1 ms) is critical for delay-sensitive machine-type communications such as traffic safety and industry processes in 5G networks [3]. SWD has lower delay since the destination only waits one extra block to decode the source information.

SWD can be joint or sequential [17], [18]. In joint decoding, the destination ($\mathcal{D}$) decodes the source ($\mathcal{S}$) information by simultaneously utilizing two received blocks. In sequential decoding, however, $\mathcal{D}$ first decodes a bin index about source information in one block and then the source information in an earlier block. Since both BD and joint SWD achieve the same rate [18], the same outage analysis is assumed [16]. However, in a block fading channel, their outage probability values differ. Moreover, in sequential decoding, there are outage events for $\mathcal{S}$ information and the bin index as well [16].

B. Related Work

In FD DF relaying over B transmission blocks, BD has a decoding delay of B blocks whereas that of SWD is one for a single relay channel [17], [18] and $n < B$ for an n-relay channel [19]. This delay stems from the superposition block Markov encoding at $\mathcal{S}$ that requires BD or SWD at $\mathcal{D}$ [17], [18]. Hence, the delay can be further reduced by switching between DT and DF relaying [5], [7], [20], or by the relay $(\mathcal{R})$ forwarding $\mathcal{S}$ information only when decoding at $\mathcal{D}$ fails as in hybrid-automatic retransmission request systems [21].

Most existing works assume HD relays including dual-hop transmission [4], DF relaying [5], [22]–[24] and partial DF relaying [7]–[9], [20], [25]–[29]. The system in Fig. 1 can achieve a full diversity order of two if it switches from DF relaying to DT when $\mathcal{R}$ goes to outage [5] or when the gain of $\mathcal{S}$-$\mathcal{D}$ link exceeds that of $\mathcal{S}$-$\mathcal{R}$ link [7], [20]. This switching requires $\mathcal{S}$ and $\mathcal{R}$ to have limited channel state information (CSI) via feedback from $\mathcal{D}$ [30]. References [31], [32] study the achievability and outage of DF relaying for multiple-antennas systems. For multiple relays, outage has been analyzed for DF relaying of a multi-hop relay network [33], single and multi-relay selection over Rayleigh [34], [35] and Nakagami-m [36] fading channels.

Outage of FD DF relaying has not been extensively analyzed except for BD considering partial DF relaying [7], coherent full DF relaying over network wide scenario [16], and independent and coherent full DF relaying [6], [37]. Full diversity order of two can be achieved when the system swithces between DT and DF relaying modes [7]. By further switching the DF mode into independent and coherent relaying, $\mathcal{R}$ can save part of its power (up to 90%) which degrades the outage performance unless $\mathcal{S}$ and $\mathcal{R}$ have full CSI [6], [37].

C. Main Results and Contributions

We investigate the FD DF relaying with BD and SWD schemes [17], [18], [38]. The link switches between DT and DF modes as in [7]. We derive the decoding delay for BD and SWD and the outage for joint and sequential SWD. Our analysis may help characterize DF relaying in network wide scenarios or in other cooperative multi-user channels such as two-way relay channel [39], cognitive radio [40] and interference channel with source cooperation [41].

As is customary [7], we assume the block fading channel model and the availability of full CSI at receivers and limited CSI at transmitters. More specifically, for any transmission block, each of $\mathcal{R}$ and $\mathcal{D}$ knows the phases and amplitudes of the channel gains. Both $\mathcal{S}$ and $\mathcal{R}$ further know the phases of their respective links to $\mathcal{D}$ which helps them perform coherent transmission. They also know the relative amplitude order between $\mathcal{S}-\mathcal{R}$ and $\mathcal{S}-\mathcal{D}$ links which helps them perform DF relaying when the $\mathcal{S}-\mathcal{R}$ link is stronger or DT when the $\mathcal{S}-\mathcal{D}$ link is stronger. $\mathcal{D}$ performs either BD, joint or sequential SWD [17], [18].

1) *Average block decoding delay* of BD and SWD are derived in closed form. The decoding delay depends on statistics of $\mathcal{S}$-$\mathcal{R}$ and $\mathcal{S}$-$\mathcal{D}$ links that determine the ratio of DT and DF mode usage. While the DT mode is delay free, the DF mode is not. Hence, the total delay depends on the average number of times for the DF mode. Results show that the decoding delay of BD increases with the number of transmission blocks, while that of SWD approaches one.
2) *Outage performances* for joint and sequential SWD are derived considering the outage events at both $\mathcal{R}$ and $\mathcal{D}$ and the channel variation over two transmission blocks. Moreover, in sequential decoding, outage events for both the bin index and $\mathcal{S}$ information are considered.
3) *Diversity orders* for joint and sequential SWD are derived considering the high SNR outage. We show that they both achieve a full diversity order of two provided that $\mathcal{S}$ allocates no more than $2^{-\text{target rate}}$ portion of its power to the new information in each transmission block.
4) *Coding gain gaps* are also derived at high SNR between sequential and joint SWD, BD scheme in [6] and HD DF scheme in [7].

Results show that FD DF relaying with BD [6], [16], [42] outperforms SWD while joint decoding outperforms sequential decoding and they both outperform HD DF relaying [7] for a wide range of SNR. However, at high SNR, HD DF relaying scheme in [7] outperforms the FD relaying with SWD.

Analysis and results illustrate the delay-outage tradeoffs between BD, SWD and HD transmission. Since 5G network supports multiple radio access technologies [2], [11], the optimal scheme for a specific service may be chosen based on its outage, throughput and delay requirements.

D. Paper Organization

The reminder of this paper is organized as follows. Section II presents the relay channel model. Section III describes the DF relaying with BD, joint and sequential SWD and derives their achievable rates. Section IV derives the average block decoding delay for BD and SWD techniques. Section V derives the DF relaying outage with joint and sequential SWD while Section VI derives their diversity orders and coding gains. Section VII presents numerical results and Section VIII concludes the paper.

II. Channel Model

The basic relay channel has one $\mathcal{S}$ communicating with $\mathcal{D}$ via $\mathcal{R}$ (Fig. 2). For FD transmission over B blocks ($B \in \mathbb{N}$ and $B \gg 1$), the received signals at block $k \in \{1, 2, ..., B\}$ are given by

$$\begin{aligned} Y_{r,k} &= h_{rs,k}X_{s,k} + Z_{r,k}, \\ Y_{d,k} &= h_{ds,k}X_{s,k} + h_{dr,k}X_{r,k} + Z_{d,k}, \end{aligned} \tag{1}$$

where $Y_{r,k}$ $(Y_{d,k})$ is the $k-$th received signal block at $\mathcal{R}$ $(\mathcal{D})$ and $Z_{r,k}$ and $Z_{d,k}$ are independent and identically distributed (i.i.d.) complex Gaussian noise terms $(\mathcal{CN}(0,1))$. $X_{s,k}$ and $X_{r,k}$ are the $k-$th signal blocks transmitted by $\mathcal{S}$ and $\mathcal{R}$, respectively. We consider block fading channel where the links remain constant in each transmission block and change independently in the next block. Hence, in block k, each link gain is modeled by Rayleigh fading and pathloss as follows:

$$\begin{aligned} h_{ij,k} &= \tilde{h}_{ij,k}/(d_{ij}^{\alpha_{ij}/2}), \\ &= g_{ij,k}e^{\sqrt{-1}\theta_{ij}},\ i \in \{r,d\},\ j \in \{s,r\} \end{aligned} \tag{2}$$

where $\tilde{h}_{ij,k} \sim \mathcal{CN}(0,1)$ represents small scale fading. The large scale fading is captured by pathloss where d_{ij} is the

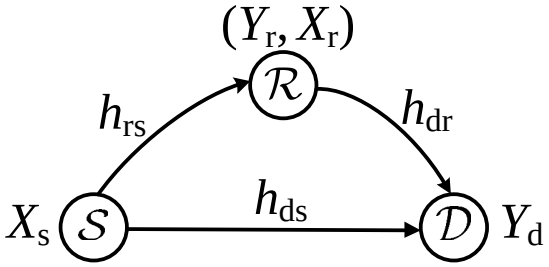

Fig. 2. Basic Relay channel model.

distance between nodes i and j and α_{ij} is the attenuation factor. Let $g_{ij,k}$ and $\theta_{ij,k}$ be the amplitude and the phase of a link coefficient in block k, respectively. Then, $g_{ij,k} = |\tilde{h}_{ij,k}|/d_{ij}^{\alpha_{ij}/2}$ is Rayleigh distributed while $\theta_{ij,k}$ is uniform in $[0, 2\pi]$. We assume full CSI at receivers and partial CSI at transmitters. This assumption implies the following. In receiving, $\mathcal{R}$ knows $h_{rs,k}$ and $\mathcal{D}$ knows $h_{ds,k}$ and $h_{dr,k}$. In transmitting, $\mathcal{S}$ knows statistical (not exact instantaneous) knowledge of the links, which is used by $\mathcal{S}$ to optimize its transmit power to minimize the outage. Moreover, $\mathcal{S}$ and $\mathcal{R}$ each knows the phase of its respective link to $\mathcal{D}$, and they both know the order between $g_{rs,k}^2$ and $g_{ds,k}^2$. The phase knowledge at transmitters is important for coherent transmission while the amplitude order knowledge determines the optimal transmission scheme as specified in Section III. The CSI at transmitters can be obtained via feedback from $\mathcal{D}$ [30].

We assume that the relay signal $Y_{r,k}$ does not have a self-interference noise term. This assumption may be justified due to the following reasons. First, efficient self-interference cancellation of up to 110 dB has been demonstrated for WiFi radios [14]. Second, since good statistical models for the residual self-interference are underdeveloped [12], it may be modeled as another source of noise. Thus, to incorporate the residual self-interference, we may increase the noise power or decrease the transmit power in (1).

We consider no external interference in this model as we focus on the fundamental outage and delay performance. In a larger setting such as in an ad hoc or cellular network, the system will be interference limited rather than noise limited. Moreover, although our delay and outage analyses may be generalized to include interference, this topic is beyond the scope of this paper.

III. DF Relaying scheme

We consider the FD DF scheme in [17], [18], [38] where the transmission is carried over B blocks ($B >> 1$, $B \in \mathbb{N}$) and $\mathcal{S}$ aims to send $B-1$ messages through B blocks[1]. However, DF relaying may not occur for all $k \in \{1, 2, ..., B\}$. Instead, DT replaces DF relaying depending on the relative channel gains of $\mathcal{S}-\mathcal{R}$ ($g_{rs,k}$) and $\mathcal{S}-\mathcal{D}$ ($g_{ds,k}$) links as in [7]. This is because when $g_{rs,k} < g_{ds,k}$, decoding at $\mathcal{R}$ may constrain the achievable rate. In order to determine the operating mode for block $k \in \{1, 2, ..., B\}$, $\mathcal{S}$ must know the relative order of $g_{rs,k}$ and $g_{ds,k}$.

[1]In the last transmission block, $\mathcal{S}$ sends only the old information (no new information). This may reduce the average achievable rate. However, this rate reduction becomes negligible as the number of blocks $B \to \infty$ [18].

Although such switching is somewhat complicated, we emphasize that only one bit feedback is needed from $\mathcal{D}$ to $\mathcal{S}$ and $\mathcal{R}$. This small non-user data (feedback information) satisfy the ultra lean design requirement for 5G networks [3], which will also support multiple radio access technologies that enable switching among different modes based on channel qualities and service requirements.

A. Direct Transmission Mode: ($g_{rs,k} \leq g_{ds,k}$)

This mode for block k occurs when $\mathcal{S}-\mathcal{R}$ link is weaker than $\mathcal{S}-\mathcal{D}$ link ($g_{rs,k} \leq g_{ds,k}$). Clearly, we have a classical point-to-point communication without $\mathcal{R}$ where $\mathcal{S}$ sends its information directly to $\mathcal{D}$ at rate $R \leq \log\left(1 + g_{ds,k}^2 P_s\right)$ as P_s is the transmit power of $\mathcal{S}$.

B. DF Relaying Mode: ($g_{rs,k} > g_{ds,k}$)

This mode for block k occurs when $\mathcal{S}-\mathcal{R}$ link is stronger than $\mathcal{S}-\mathcal{D}$ link ($g_{rs,k} > g_{ds,k}$). This scheme uses superposition block Markov encoding [[18], Chapter 16] where $\mathcal{R}$ decodes $\mathcal{S}$ information in block k (w_k) and then forwards it coherently with $\mathcal{S}$ to $\mathcal{D}$ in block $m > k$ in which the $\mathcal{S}-\mathcal{R}$ link is also stronger than $\mathcal{S}-\mathcal{D}$ link ($g_{rs,m} > g_{ds,m}$). $\mathcal{D}$ then utilizes the signals received from $\mathcal{S}$ and $\mathcal{R}$ and performs either BD or SWD for w_k.

1) Transmission Scheme: Assume that $\mathcal{S}-\mathcal{R}$ link is stronger than $\mathcal{S}-\mathcal{D}$ link in blocks v, k and m where $v < k < m$ and $(v, k, m) \in \{1, 2, ..., B\}$. In block k, $\mathcal{S}$ uses superposition coding to encode its new information (w_k) with the old information (w_v) sent in block v. $\mathcal{S}$ then transmits the signal that conveys this superposed codeword (for w_k and w_v). Next, in block k, $\mathcal{R}$ decodes w_k and transmits the signal of its codeword (for w_k) in block m.

2) Transmit Signals: $\mathcal{S}$ and $\mathcal{R}$ respectively construct their Gaussian transmit signals as follows:

$$X_{s,k} = \sqrt{\rho_1}U_1(w_k) + \sqrt{\rho_2}U_2(w_v),\ X_{r,k} = \sqrt{P_r}U_2(w_v) \quad (3)$$

where $U_j \sim N(0,1)$ for $j \in \{1, 2\}$. Codeword U_1 conveys new information w_k while U_2 conveys old information w_v. Here, $\mathcal{R}$ allocates its power P_r for the signal U_2 while $\mathcal{S}$ allocates the transmission powers ρ_1 and ρ_2 for signals U_1 and U_2, respectively. The power allocation parameters (ρ_1, ρ_2) satisfy the power constraint $\rho_1 + \rho_2 = P_s$.

3) Decoding: The decoding at $\mathcal{R}$ is straightforward where in block k, $\mathcal{R}$ already knows w_v from the decoding in block v and it can reliably decode w_k at the following rate:

$$R \leq \log\left(1 + g_{rs,k}^2 \rho_1\right) = C_1. \quad (4)$$

$\mathcal{D}$ decodes $\mathcal{S}$ information using BD, joint or sequential SWD as follows:

Backward Decoding (BD): In this decoding, $\mathcal{D}$ decodes w_v in block k given that it knows w_k from the decoding in block m. $\mathcal{D}$ then can reliably decode w_v at the following rate [18]:

$$R \leq \log\left(1 + g_{ds,k}^2 P_s + g_{dr,k}^2 P_r + 2g_{ds,k}g_{dr,k}\sqrt{\rho_2 P_r}\right) = C_2. \quad (5)$$

From (4) and (5), the achievable rate with BD is given as follows:

$$R \leq \min\{C_1, C_2\}, \quad (6)$$

Joint Sliding Window Decoding (SWD): Here, $\mathcal{D}$ decodes w_k from the received signals in blocks k and m $(Y_{d,k}, Y_{d,m})$ given that it already knows w_v from the previous decoding step (from signals $Y_{d,v}$ and $Y_{d,k}$). The reliable rate for w_k at $\mathcal{D}$ is given as follows [17], [38]:

$$\begin{aligned} R \leq & \log(1+g_{ds,k}^2\rho_1) \\ & + \log\left(1+\frac{g_{ds,m}^2\rho_2 + g_{dr,m}^2 P_r + 2g_{ds,m}g_{dr,m}\sqrt{\rho_2 P_r}}{1+g_{ds,m}^2\rho_1}\right) \\ & = C_3. \end{aligned} \tag{7}$$

From (4) and (7), the achievable rate with joint decoding is given as follows:

$$R \leq \min\{C_1, C_3\}, \tag{8}$$

Remark 1. Formulas (6) and (8) show that SWD achieves the same rate for each source message as BD in AWGN channels, but with much shorter decoding delay since $C_2 = C_3$ as $g_{ds,k} = g_{ds,m}$. However, the two decoding schemes are not equivalent in fading channels since $C_2 \neq C_3$ as $g_{ds,k} \neq g_{ds,m}$ which can lead to different outages. Moreover, although both BD and SWD in fading achieve the same average sum rate for all $B-1$ messages sent in all B blocks, each message experiences different outage because of channel variation over different blocks.

Sequential Sliding Window Decoding: Another scheme called DF via binning was proposed in [18]. In this scheme, $\mathcal{S}$ messages are sorted into equal size groups and a bin index (l) is given for each group. Then, in each block, $\mathcal{S}$ sends the new message and the bin index of the previous message (l_v). $\mathcal{R}$ decodes the new message in one block and forwards the bin index of that message in the next block. The transmit signals for this scheme are similar to (3) but replacing each w_v by l_v. $\mathcal{D}$ performs sequential decoding where it first utilizes its received signal in block m to decode l_k at the following rate:

$$\begin{aligned} R_b \leq & \log\left(1+\frac{g_{ds,m}^2\rho_2 + g_{dr,m}^2 P_r + 2g_{ds,m}g_{dr,m}\sqrt{\rho_2 P_r}}{1+g_{ds,m}^2\rho_1}\right) \\ & = C_4, \end{aligned} \tag{9}$$

where R_b is the transmission rate for the bin index l_k which is less than the transmission rate R $(R_b \leq R)$. $\mathcal{D}$ next goes back to block k and decodes the transmit information w_k, given that it knows l_v and l_k where $w_k \in l_k$, at the following rate:

$$R - R_b \leq \log(1+g_{ds,k}^2\rho_1) = C_5. \tag{10}$$

Then, from (4), (9) and (10), the achievable rate with sequential decoding is given as in (8).

Remark 2. Unlike joint decoding, sequential decoding simplifies the decoding at $\mathcal{D}$ but complicates the encoding at $\mathcal{S}$ and $\mathcal{R}$ since they need to group the information into bins and determine the optimal binning index rate.

Remark 3. Although achieving the same rate, the outage probabilities of joint and sequential SWD are different. In joint decoding, $\mathcal{D}$ decodes $\mathcal{S}$ information w_k using the received blocks k and m simultaneously. However, in sequential decoding, $\mathcal{D}$ first decodes the bin index l_k in block m and then w_k in block k. The outages for these 2 schemes are derived in Section V.

IV. Average Block Decoding Delay

Throughput and low latency are specified for applications in 5G networks [3]. For instance, traffic safety requires an end-to-end latency of 1 ms or less [3], but vehicular telematics can tolerate a latency of 1 s [43]. Hence, the optimal transmission scheme depends on the application requirements.

Although FD relaying achieves significantly better rates than HD relaying [11], the latter has no decoding delay since the decoding is performed at the end of each transmission block [7]. In contrast, FD relaying has at least one block decoding delay when using SWD. Hence, a rate-delay trade-off exists between FD and HD DF relaying schemes.

In this section, we derive the average decoding delay for both BD and SWD. For these schemes, the delay occurs only in DF mode since in DT mode, $\mathcal{D}$ decodes $\mathcal{S}$ information at the end of a transmission block. Hence, the average decoding delay depends on the decoding technique and channel statistics that determine the ratio between DT and DF modes.

A. Backward Decoding (BD)

Here, the decoding delay for block $k \in \{1, 2, ..., B\}$ is either 0 during DT mode or $B-k$ during DF relaying mode. Therefore, the decoding delay T_k^{BD} for any transmission block k is given as follows:

$$\begin{aligned} T_k^{BD} &= \mathsf{P}[g_{rs,k} \leq g_{ds,k}] \times 0 + \mathsf{P}[g_{rs,k} > g_{ds,k}] \times (B-k), \\ &\overset{(a)}{=} \frac{\mu_{rs}}{\mu_{rs}+\mu_{ds}}(B-k), \end{aligned} \tag{11}$$

where (a) is obtained by using the Rayleigh distribution of $g_{ds,k}$, and $g_{rs,k}$ as shown in [[27], Proof of Lemma 2]. $\mu_i = E[g_i^2]$ is the mean of g_i^2 for $i \in \{ds, dr, rs\}$. The following theorem yields the average decoding delay $\overline{T}^{BD}$.

Theorem 1. *The average decoding delay for FD DF relaying with BD* $(\overline{T}^{BD})$ *is given by:*

$$\overline{T}^{BD} = 0.5B\left(\mu_{rs}/(\mu_{rs}+\mu_{ds})\right). \tag{12}$$

Proof. Obtained by summing T_k^{BD} in (11) over all $k \in \{1, 2, ..., B-1\}$, dividing the summation over $B-1$ and then using the summation identity $\sum_{k=1}^{n} k = 0.5n(n+1)$ as shown in Appendix A.1. □

Theorem 1 shows that the delay increases as the number of blocks (B) increases, thus limiting the usefulness of BD for delay sensitive applications although it has better outage than SWD as shown in Sections VI and VII.

B. Sliding Window Decoding

The average decoding delays of SWD for both joint and sequential methods are identical as $\mathcal{D}$ utilizes two received blocks to decode $\mathcal{S}$ information. The delay for the k^{th} block is 0 for DT mode and varies from 1 to $B-k$ during DF mode depending on subsequent channel realizations after block k that determine the DT and DF modes. For example, the decoding delay for $\mathcal{S}$ information in block 4 (w_4) is 2 if $g_{rs,4} > g_{ds,4}$, $g_{rs,5} < g_{ds,5}$ and $g_{rs,6} > g_{ds,6}$ since $\mathcal{D}$ will wait till block 6 to decode w_4. However, if $g_{rs,k} > g_{ds,k}$ and $g_{rs,n} \leq g_{ds,n}$ for all $k < n < B-k-1$, the decoding

delay then is $B-k$ as $\mathcal{R}$ will forward w_k in the last block B regardless of the link order in block B. Generally, the decoding delay T_k^{SWD} for any transmission block k is given as follows:

$$T_k^{SWD} = \mathsf{P}[g_{rs,k} \le g_{ds,k}] \times 0 + \mathsf{P}[g_{rs,k} > g_{ds,k}] \times P^*,$$
$$P^* = \sum_{i=1}^{B-(k+1)} i\mathsf{P}[g_{rs,k+i} > g_{ds,k+i}] \prod_{n=1}^{i-1} \mathsf{P}[g_{rs,k+n} < g_{ds,k+n}] + (B-k) \prod_{n=1}^{B-k-1} \mathsf{P}[g_{rs,k+n} < g_{ds,k+n}]. \quad (13)$$

By using Rayleigh distributions, T_k^{SWD} becomes as follows:

$$T_k^{SWD} = \frac{\mu_{rs}}{\mu_{rs}+\mu_{ds}} \left[\sum_{i=1}^{B-(k+1)} i \times \frac{\mu_{ds}^{i-1}\mu_{rs}}{(\mu_{ds}+\mu_{rs})^i} + (B-k)\left(\frac{\mu_{ds}}{\mu_{ds}+\mu_{rs}}\right)^{B-k-1} \right]. \quad (14)$$

The average decoding delay $\overline{T}^{SWD}$ is then given as follows:

Theorem 2. *The average decoding delay for FD DF relaying with joint or sequential SWD ($\overline{T}^{SWD}$) is given as follows:*

$$\overline{T}^{SWD} = 1 - \frac{\mu_{ds}}{\mu_{rs}(B-1)} \left[1 - \left(\frac{\mu_{ds}}{\mu_{ds}+\mu_{rs}} \right)^{B-1} \right]. \quad (15)$$

Proof. Sum T_k^{SWD} in (13) over all $k \in \{1, 2, ..., B-1\}$, divide over $B-1$ and then use the identity $\sum_{k=1}^{n} x^k = x(x^n - 1)(x-1)^{-1}$ as shown in Appendix A.2. □

Theorem 2 shows two reasons for preferring SWD over BD for delay sensitive applications. First, the SWD decoding delay approaches one as the number of blocks approaches infinity ($B \to \infty$). This is because if the message in block k is through DF relaying mode and $\mathcal{D}$ decodes it in block m, the decoding delay for this message is $m-k$ while the decoding delays for other messages sent in blocks $k+1, k+2, ..., m$ are zero which makes the average equal to one.

Second, for a message sent in block k, formula (13) implies that the probability of decoding this message in block $m > k$ decreases as m increases since the event of this probability occurs when $g_{rs,k} > g_{ds,k}$, $g_{rs,m} > g_{ds,m}$ and $g_{rs,i} < g_{ds,i}$ for all $i \in \{k+1, k+2, ..., m-1\}$. In contrast, in BD, the message sent in block k will be decoded after $B-k$ blocks when $g_{rs,k} > g_{ds,k}$ that occurs with $\mu_{rs}/(\mu_{rs}+\mu_{ds})$ probability.

V. Outage for Sliding Window Decoding

Many wireless applications tolerate a maximum outage percentage (e.g., 2% for VoIP service in LTE release 8 [44]). Since the outage of BD is derived in [7], [16], [42], we derive here the outage of FD DF relaying with joint and sequential SWD by considering both DT and DF modes over two blocks.

A. Joint Sliding Window Decoding

The outage is related to the achievable rate for DT mode in Section III-A and DF modes given in (4) and (7). We analyze the outage as follows. Define $\mathbb{P}_1$ and $\mathbb{P}_2$ as outage for DT and DF modes, respectively. The average outage probability ($\bar{\mathbb{P}}_o^{JSWD}$) can then be obtained as follows:

Theorem 3. *For a given target rate R with specific power allocation (ρ_1, ρ_2), the average outage probability ($\bar{\mathbb{P}}_o^{JSWD}$) of the FD DF scheme with joint SWD is given as follows:*

$$\bar{\mathbb{P}}_o^{JSWD} = \mathbb{P}_1 + \mathbb{P}_2 = \mathbb{P}_1 + \mathbb{P}_r + \mathbb{P}_d, \quad (16)$$
$$\text{with } \mathbb{P}_1 = \mathsf{P}[R > \log\left(1 + g_{ds,k}^2\rho_1\right),\ g_{rs,k} \le g_{ds,k}],$$
$$\mathbb{P}_r = \mathsf{P}\left[R > C_1,\ g_{rs,k} > g_{ds,k}\right],$$
$$\mathbb{P}_d^{JSWD} = \mathsf{P}\big[R > C_3,\ R \le C_1,\ g_{rs,k} > g_{ds,k}\big],\ where$$

- $\mathbb{P}_1$ *is the outage during DT mode,*
- $\mathbb{P}_r$ *and* $\mathbb{P}_d^{JSWD}$ *are the outages during DF mode,*
  - $\mathbb{P}_r$ *is the outage at* $\mathcal{R}$*;*
  - $\mathbb{P}_d^{JSWD}$ *is the outage at* $\mathcal{D}$ *when there is no outage at* $\mathcal{R}$*.*

Proof. From the outage events in DT and DF modes when R is higher than the achievable rate in (4) and (7). □

$\mathbb{P}_1, \mathbb{P}_r$ and $\mathbb{P}_d^{JSWD}$ can be analytically expressed as follows:

Lemma 1. *The probabilities $\mathbb{P}_1$, $\mathbb{P}_r$ and $\mathbb{P}_d^{JSWD}$ in Theorem 3 can be expressed as follows:*

$$\mathbb{P}_1 = 1 - e^{\frac{-\eta_0^2}{\mu_{ds}}} - \frac{\mu_{rs}}{\mu_{rs}+\mu_{ds}}\left(1 - e^{\frac{-\eta_0^2(\mu_{rs}+\mu_{ds})}{\mu_{rs}\mu_{ds}}}\right),$$
$$\mathbb{P}_r = 1 - e^{\frac{-\eta_2^2}{\mu_{rs}}} - \frac{\mu_{ds}}{\mu_{rs}+\mu_{ds}}\left(1 - e^{\frac{-\eta_1^2(\mu_{rs}+\mu_{ds})}{\mu_{rs}\mu_{ds}}}\right),$$
$$\mathbb{P}_d^{JSWD} = e^{-\frac{\eta_2^2}{\mu_{rs}}} \times \begin{cases} \int_0^{\eta_2}\int_0^{\zeta_2} f(\gamma_1,\beta_1,\zeta_1)d\beta_1 d\gamma_1, & \text{if } \frac{P_s}{\rho_1} > 2^R \\ \int_0^{\eta_1}\int_0^{\infty} f(\gamma_1,\beta_1,\zeta_1)d\beta_1 d\gamma_1 & \\ + \int_{\eta_1}^{\eta_2}\int_0^{\zeta_2} f(\gamma_1,\beta_1,\zeta_1)d\beta_1 d\gamma_1, & \text{if } \frac{P_s}{\rho_1} \le 2^R \end{cases}, \quad (17)$$

where

$$\eta_0 = \sqrt{\frac{2^R-1}{P_s}},\ \eta_1 = \sqrt{\frac{2^R}{P_s} - \frac{1}{\rho_1}},\ \eta_2 = \sqrt{\frac{2^R-1}{\rho_1}},$$
$$\zeta_1 = P_r^{-0.5}\left(\sqrt{\delta} - \beta_1\sqrt{\rho_2}\right),\ \zeta_2 = \sqrt{\frac{2^R - (1+\gamma_1^2\rho_1)}{P_s(1+\gamma_1^2\rho_1) - 2^R\rho_1}}$$
$$\delta = \left(1 + \beta_1^2\rho_1\right)\left(\frac{2^R}{1+\gamma_1^2\rho_1} - 1\right),$$
$$f(\gamma_1,\beta_1,\zeta_1) = \frac{4\gamma_1\beta_1}{\mu_{ds}^2} e^{-\frac{\gamma_1^2+\beta_1^2}{\mu_{ds}}}\left(1 - e^{-\frac{\zeta_1^2}{\mu_{dr}}}\right) \quad (18)$$

Proof. $\mathbb{P}_1$, $\mathbb{P}_r$ are derived in [[6], Theorem 4] while $\mathbb{P}_d^{JSWD}$ is obtained using the Rayleigh statistics of $g_{ds,k}$, $g_{ds,m}$, $g_{rs,k}$, $g_{dr,k}$, and $g_{dr,m}$ as shown in Appendix B. □

Remark 4. We obtain numerically the optimal resource allocation (ρ_1, ρ_2) that minimizes $\bar{\mathbb{P}}_o^{JSWD}$ since Theorem 3 specifies the outage for a fixed resource allocation.

B. Sequential Sliding Window Decoding

The outage here is similar to that of joint decoding except for the outage at $\mathcal{D}$ during the DF mode. In sequential SWD, an outage at $\mathcal{D}$ can occur not only for $\mathcal{S}$ information (w) but also for the bin index (l). An outage for l leads to an outage for w since each l represents a group of w ($w \in l$). The average outage probability ($\bar{\mathbb{P}}_o^{SSWD}$) can be obtained as follows:

Theorem 4. *For a given target rate R with specific resource allocation (power (ρ_1, ρ_2) and binning rate (R_b)), the average outage probability $(\bar{\mathbb{P}}_o^{SSWD})$ of the FD DF scheme with sequential SWD is given as in Theorem 3 except replacing $\mathbb{P}_d^{JSWD}$ by $\mathbb{P}_d^{SSWD}$, which is given as follows:*

$$\mathbb{P}_d^{SSWD} = \mathbb{P}_{d1} + \mathbb{P}_{d2}, \text{ where} \quad (19)$$
$$\mathbb{P}_{d1} = \big[R_b > C_4,\ R \le C_1,\ g_{rs,k} > g_{ds,k}\big],$$
$$\mathbb{P}_{d2} = \big[R - R_b > C_5,\ R_b \le C_4,\ R \le C_1,\ g_{rs,k} > g_{ds,k}\big].$$

- *$\mathbb{P}_{d1}$ is the outage probability of the bin index (l) at $\mathcal{D}$ when there is no outage at $\mathcal{R}$,*
- *$\mathbb{P}_{d2}$ is the outage probability of $\mathcal{S}$ information (w) at $\mathcal{D}$ when there is no outage at $\mathcal{R}$ for w or at $\mathcal{D}$ for l.*

$\mathbb{P}_{d1}$ and $\mathbb{P}_{d2}$ can be analytically expressed as follows:

$$\mathbb{P}_{d1} = \left(e^{-\frac{\eta_2^2}{\mu_{rs}}} - \frac{\mu_{ds}}{\mu_{ds}+\mu_{rs}} e^{-\frac{\eta_2^2(\mu_{ds}+\mu_{rs})}{\mu_{ds}\mu_{rs}}}\right) \times \begin{cases} \int_0^{\zeta_4} f_1(\beta_1,\zeta_3)d\beta_1, & \text{if } \frac{P_s}{\rho_1} > 2^{R_b} \\ \int_0^{\infty} f_1(\beta_1,\zeta_3)d\beta_1, & \text{if } \frac{P_s}{\rho_1} \le 2^{R_b} \end{cases} \quad (20)$$

$$\mathbb{P}_{d2} = e^{-\frac{\eta_2^2}{\mu_{rs}}}\left(1 - e^{-\frac{\eta_3^2}{\mu_{ds}}}\right) \times \begin{cases} e^{-\frac{\zeta_4^2}{\mu_{ds}}} + \int_0^{\zeta_4} f_2(\beta_1,\zeta_3)d\beta_1, & \text{if } \frac{P_s}{\rho_1} > 2^{R_b} \\ \int_0^{\infty} f_2(\beta_1,\zeta_3)d\beta_1, & \text{if } \frac{P_s}{\rho_1} \le 2^{R_b} \end{cases}$$

$$\text{where } \eta_3 = \sqrt{\frac{2^{R-R_b}-1}{\rho_1}}, \quad \zeta_4 = \sqrt{\frac{2^{R_b}-1}{P_s - 2^{R_b}\rho_1}},$$
$$\zeta_3 = P_r^{-0.5}\left(\sqrt{(2^{R_b}-1)(1+\beta_1^2\rho_1)} - \beta_1\sqrt{\rho_2}\right),$$
$$f_1(\beta_1,\zeta_3) = \frac{2\beta_1}{\mu_{ds}} e^{-\frac{\beta_1^2}{\mu_{ds}}}\left(1 - e^{-\frac{\zeta_3^2}{\mu_{dr}}}\right),$$
$$f_2(\beta_1,\zeta_3) = \frac{2\beta_1}{\mu_{ds}} e^{-\left(\frac{\beta_1^2}{\mu_{ds}} + \frac{\zeta_3^2}{\mu_{dr}}\right)} \quad (21)$$

Proof. See Appendix C. □

Remark 5. As in Theorem 3, we numerically optimize resource allocation (ρ_1, ρ_2, R_b) that minimizes $\bar{\mathbb{P}}_o^{SSWD}$.

As per Remark 2, compared with joint decoding, sequential decoding simplifies the decoding at $\mathcal{D}$ but has another variable (R_b) to be optimized. Moreover, joint decoding outperforms sequential decoding as shown in the following Lemma:

Lemma 2. *For a given target rate R with specific resource allocation $(\rho_1, \rho_2$ and $R_b)$, The outage gap between joint and sequential SWD decoding is given as follows:*

$$\bar{\mathbb{P}}_o^{SSWD} - \bar{\mathbb{P}}_o^{JSWD} = \mathsf{P}\big[R_b > C_4,\ R \le C_3,\ \xi\big] + \mathsf{P}\big[R_b \le C_4,\ R > C_5 + R_b,\ R \le C_3,\ \xi\big] \ge 0, \quad (22)$$

where ξ is the event that $R \le C_1,\ g_{rs,k} > g_{ds,k}$ and C_1, C_4 and C_5 are given in Section III.B.

Proof. Obtained by comparing $\mathbb{P}_d^{JSWD}$ and $\mathbb{P}_d^{SSWD} = \mathbb{P}_{d1} + \mathbb{P}_{d2}$ since $\mathbb{P}_1$ and $\mathbb{P}_r$ are the same for both techniques. Since $C_3 = C_4 + C_5$ as shown in (7),(9) and (10), $\mathbb{P}_d^{JSWD}$ in (16) and $\mathbb{P}_{d1}$ and $\mathbb{P}_{d2}$ in (19) can be expressed as follows:

$$\mathbb{P}_d^{JSWD} = \mathsf{P}\big[R_b > C_4,\ R > C_3, \xi\big] + \mathsf{P}\big[R_b \le C_4,\ R > C_3, \xi\big],$$
$$\mathbb{P}_{d1} = \mathsf{P}\big[R_b > C_4,\ R > C_3,\ R \le C_3,\ \xi\big],$$
$$\mathbb{P}_{d2} = \mathsf{P}\big[R - R_b > C_5,\ R_b \le C_4,\ R > C_3,\ R \le C_3,\ \xi\big],$$

Then, from $\mathbb{P}_d^{JSWD} - \mathbb{P}_d^{SSWD}$, we obtain (22). □

VI. Asymptotic Performance at high SNR

While the analysis in Section V determines the outage at any SNR, analyzing the asymptotic performance at high SNR simplifies the diversity order analysis of SWD and allows easier comparison with BD [7], [16], [42].

A. Diversity Order

Before formal derivation, we intuitively see from (16) and (19) that the diversity order is two for joint and sequential SWD since both DT and DF relaying modes require at least two different links to fade for an outage at $\mathcal{R}$ or $\mathcal{D}$. More specifically, for both joint and sequential SWD, an outage occurs at $\mathcal{D}$ in DT mode when both $g_{ds,k}$ and $g_{rs,k}$ are faded as deduced from $\mathbb{P}_1^{JSWD}$ in (16). The same holds for the outage at $\mathcal{R}$ in DF relaying mode considering $\mathbb{P}_r^{JSWD}$ in (16). For joint SWD, an outage at $\mathcal{D}$ in DF relaying mode occurs when $g_{ds,k}$, $g_{ds,m}$ and $g_{dr,m}$ are faded as deduced from $\mathbb{P}_d^{JSWD}$ in (16). For sequential SWD, on the one hand, $\mathbb{P}_{d2}$ in (19) can be reduced to zero by setting $R_b = R$ since at high SNR, $\mathcal{R}$ has enough power to transmit the decoded information and there is no need to bin $\mathcal{S}$ messages into groups. On the other hand, from (19), C_4 in $\mathbb{P}_{d1}$ is maximized when $\rho_1 \to 0$. Hence, an outage occurs when both $g_{ds,m}$ and $g_{dr,m}$ are faded.

Without loss of generality, assume equal transmit powers from $\mathcal{S}$ and $\mathcal{R}$ $(P_s = P_r = P)$ and define a nominal SNR $= \mu_{ds}P$ as the received power at $\mathcal{D}$ in DT mode. Note that this SNR is always proportional to P. Hence, to prove that the diversity order is two, we show that the dominant term of outage is proportional to P^{-2} [45], [46].

Theorem 5. *For full-duplex DF relaying with joint or sequential SWD, the diversity order is two since the outage probabilities for joint $(\mathbb{P}_{o,\infty}^{JSWD})$ and sequential $(\mathbb{P}_{o,\infty}^{SSWD})$ SWD at high-SNR respectively approach the following values:*

$$\mathbb{P}_{o,\infty}^{JSWD} = J_1 P^{-2}, \quad \mathbb{P}_{o,\infty}^{SSWD} = J_2 P^{-2}, \quad (23)$$
$$J_1 = \frac{(2^R-1)^2(1+2^{2R})}{2\mu_{ds}\mu_{rs}},$$
$$J_2 = \frac{(2^R-1)^2}{2\mu_{ds}}\Big(\mu_{rs}^{-1}(1+a_1^{-2}) + \frac{\mu_{rs}\kappa^2}{(\mu_{ds}+\mu_{rs})(1-a_1 2^R)^2}\Big),$$
$$\kappa = \sqrt{a_1(2^R-1)} - \sqrt{1-a_1}, \text{ for } a_1 <\in (0, 2^{-R}).$$

Sketch of the Proof:. From [[6], Corollary 1], we obtain $\mathbb{P}_{1,\infty}$ and $\mathbb{P}_{r,\infty}$ as follows:

$$\mathbb{P}_{1,\infty} = \frac{(2^R-1)^2}{2\mu_{ds}\mu_{rs}}P^{-2}, \ \mathbb{P}_{r,\infty} = \frac{(2^R-1)^2}{2\mu_{ds}\mu_{rs}a_1^2}P^{-2}. \quad (24)$$

Then, for joint SWD, using the first order Taylor series expansion $e^{-x} = 1 - x$ in (17), Appendix D shows that $\mathbb{P}_{d,\infty}^{JSWD}$ is given as follows:

$$\mathbb{P}_{d,\infty}^{JSWD} = \begin{cases} \frac{1}{2\mu_{ds}^2\mu_{dr}a_1^2P^3}K_1, & \text{if } \frac{P_s}{\rho_1} > 2^R \\ \frac{2^R}{\mu_{ds}P}(1-K_2), & \text{if } \frac{P_s}{\rho_1} \le 2^R \end{cases}, \quad (25)$$

where a_1 and a_2 are the power ratios defined as

$$a_1 = \rho_1/P, \quad a_2 = \rho_2/P = 1 - a_1, \quad \{a_1, a_2\} \in (0,1),$$

and K_1, and K_2 are constants that depend on the power ratios (a_1, a_2), target rate (R) and the average channel gains. They are expressed as follows:

$$K_1 = \int_{a_1(2^R-1)^{-1}}^{\infty} \frac{(\sqrt{2^R x - a_1} - \sqrt{a_2})^2((2^R-1)x - a_1)^2}{x^2\left(\left(a_1^{-1} - 2^R\right)x + 1\right)^2} dx,$$

$$K_2 = \int_{a_2}^{\infty} \frac{\mu_{dr}}{(x+a_1)^2\left(\mu_{dr} + \mu_{ds}(\sqrt{x} - \sqrt{a_2})^2\right)} dx, \quad (26)$$

Hence, $\mathbb{P}_{d,\infty}^{JSWD} \propto P^{-3}$ only when $a_1 < 2^{-R}$, otherwise $\mathbb{P}_{d,\infty}^{JSWD} \propto P^{-1}$. However, deceasing a_1 will increase the outage at $\mathcal{R}$ $(\mathbb{P}_{r,\infty})$. Therefore, to minimize the outage, we set $a_1^* \to 2^{-R}$. Then, we obtain $\mathbb{P}_{o,\infty}^{JSWD}$ as in (23).
Similarly, for sequential SWD, using the first order Taylor series expansion $e^{-x} = 1 - x$ in (20), Appendix E shows that $\mathbb{P}_{d,\infty}^{SSWD}$ is given as follows:

$$\mathbb{P}_{d1,\infty}^{SSW} = \frac{\mu_{rs}}{\mu_{ds} + \mu_{rs}} \times \begin{cases} \frac{(2^R-1)^2\left(\sqrt{a_1(2^R-1)} - \sqrt{a_2}\right)^2}{2\mu_{ds}(1-a_1 2^R)^2 P^2}, & \text{if } \frac{P_s}{\rho_1} > 2^{R_b} \\ 1 - \frac{\mu_{dr}}{\mu_{dr} + \left(\sqrt{(2_b^R-1)a_1} - \sqrt{a_2}\right)^2 \mu_{ds}}, & \text{if } \frac{P_s}{\rho_1} \le 2^{R_b} \end{cases} \quad (27a)$$

$$\mathbb{P}_{d2,\infty}^{SSW} = \frac{2^{R-R_b} - 1}{\mu_{ds} a_1 P} \times \begin{cases} 1, & \text{if } \frac{P_s}{\rho_1} > 2^{R_b} \\ \frac{\mu_{dr}}{\mu_{dr} + \left(\sqrt{(2_b^R-1)a_1} - \sqrt{a_2}\right)^2 \mu_{ds}}, & \text{if } \frac{P_s}{\rho_1} \le 2^{R_b} \end{cases} \quad (27b)$$

Then, by setting $a_1 < 2^{-R}$ and $R_b = R$, $\mathbb{P}_{d1,\infty}^{SSW} \propto 1/P^2$ in (27a) while $\mathbb{P}_{d2,\infty}^{SSW} = 0$ in (27b), respectively. □

Theorem 5 implies that the full-diversity order of two is achieved by SWD provided that $\mathcal{S}$ allocates no more than 2^{-R} portion of its power to the new information sent in DF mode for both joint and sequential decoding. Moreover, $\mathcal{R}$ allocates a different bin index for each message $(R_b = R)$ in sequential decoding scheme, which is equivalent to no binning.

The first constraint $(a_1 < 2^{-R})$, considering C_3 in (7) and C_4 in (9), reduces the interference at $\mathcal{D}$ caused by the new information when decoding the old information (bin index) in joint (sequential) SWD. However, while this constraint decreases the outage at $\mathcal{D}$, it increases the outage at $\mathcal{R}$. Hence, the outage at $\mathcal{R}$ becomes dominant in DF mode.

The other condition $(R_b = R)$ for sequential SWD implies that at high SNR, $\mathcal{R}$ sends $\mathcal{S}$ information (no binning) and $\mathcal{D}$ decodes it through one block instead of two blocks. More specifically, it is sufficient for $\mathcal{D}$ to directly decode the old information w_k in block m instead of the bin index l_k in block m and then w_k in block k.

B. Coding gains gaps

The coding gain gap is the SNR gap between two schemes that is required to achieve the same outage performance. Having the outage expressions at high SNR in Theorem 5 for joint and sequential SWD, in [[6], Corollary 1] for BD and in [[7], Theorem 3] for HD transmission, we can derive some coding gain gaps as follows.

1) SNR gap between BD [6] and joint SWD: To achieve the same performance of BD, the SNR in joint SWD should be increased by the following gap:

Lemma 3. *For the same outage at high SNR, the SNR gap Γ_1 (in dB) between BD and joint SWD is given as follows:*

$$\Gamma_1 = \textit{SNR}_{\textit{JSWD}} - \textit{SNR}_{\textit{BD}} = 5\log(1 + 2^{2R}) - 5\log(\vartheta_1), \quad (28)$$

where

$$\vartheta_1 = 1 + (a_1^*)^{-2} + \frac{\mu_{rs}}{\mu_{dr}}\left(\sqrt{(1-a_1^*)/(-a_1^*)}\sinh^{-1}\sqrt{-a_1^*} + 1\right),$$

and $a_1^* \in (0,1)$ is the solution for $f_1(a_1) = 0$ given as

$$f_1(a_1) = \frac{0.5}{\mu_{dr} a_1^2 \sqrt{\frac{1-a_1}{-a_1}}}\sinh^{-1}\sqrt{-a_1} - \frac{0.5}{\mu_{dr} a_1} - \frac{2}{\mu_{rs} a_1^3}.$$

Proof. Obtained by comparing the outage of joint SWD in Lemma 5 with that of BD given in [[6], Corollary 1] as:

$$\mathbb{P}_{o,\infty}^{BD} = \frac{(2^R-1)^2}{2\mu_{ds}\mu_{rs}} P^{-2} + \frac{(2^R-1)^2}{2\mu_{ds}\mu_{rs} a_1^2} P^{-2} + \frac{(2^R-1)^2}{2\mu_{ds}\mu_{dr}} P^{-2}\left(\sqrt{(a_1-1)/a_1}\sinh^{-1}\left(\sqrt{-a_1}\right) + 1\right). \quad (29)$$

Then, by setting $\frac{\partial \mathbb{P}_{o,\infty}^{BD}}{\partial a_1} = 0 \Leftrightarrow f_1(a_1) = 0$, we obtain a_1^* that minimizes $\mathbb{P}_{o,\infty}^{BD}$. Last, by setting $10\log(\mathbb{P}_{o,\infty}^{SWD}) = 10\log(\mathbb{P}_{o,\infty}^{BD})$, we obtain the SNR gap in (28). □

2) SNR gap between joint and sequential SWD: To achieve the same performance of joint SWD, the SNR in sequential SWD should be increased by the following gap:

Lemma 4. *For the same outage at high SNR, the SNR gap Γ_2 (in dB) between joint and sequential SWD is given as follows:*

$$\Gamma_2 = \textit{SNR}_{\textit{SSWD}} - \textit{SNR}_{\textit{JSWD}} = 5\log(\vartheta_2) - 5\log(1 + 2^{2R}), \quad (30)$$

where $\vartheta_2 = 1 + (a_1^\star)^{-2} + \frac{\mu_{rs}^2}{\mu_{ds} + \mu_{rs}} \frac{\kappa^2}{\left(1 - a_1^\star 2^R\right)^2}$,

and $a_1^\star \in (0, 2^{-R})$ is the solution for $f_2(a_1) = 0$ given as

$$f_2(a_1) = \frac{1}{\mu_{rs} a_1^3} - \frac{\mu_{rs}}{\mu_{ds} + \mu_{rs}} \times \frac{\kappa\left((1 - a_1 2^R)\left(\frac{2^R-1}{2\sqrt{a_1(2^R-1)}} + \frac{1}{2\sqrt{a_2}}\right) + 2^R\kappa\right)}{\left(1 - a_1 2^R\right)^3}$$

where κ is given in (23)

Proof. Following similar analysis in Lemma 3 but replacing $\mathbb{P}_{o,\infty}^{BD}$ with $\mathbb{P}_{o,\infty}^{SSWD}$ in (23). □

As a simpler expression, Γ_2 is upper bounded as follows:

Proposition 1. *The SNR gap Γ_2 in Lemma 4 is upper bounded as follows:*

$$\Gamma_2 < 5\log\left(1 + \frac{\mu_{rs}}{2^R(1 + 2^{2R})(2^R - 1)}\right), \quad (31)$$

Proof. Obtained from limits of J_2 in (23) when $a_1 \to 2^{-R}$ ($\lim_{a_1 \to 2^{-R}} J_2$) and since $\mu_{rs}^2/(\mu_{ds}+\mu_{rs}) < \mu_{rs}$. □

Remark 6. The SNR gap (Γ_3) between BD and sequential SWD is the sum of Γ_1 and Γ_2.

3) SNR gap between joint SWD and HD DF scheme [7]: Similar to Lemmas 3 and 4, the SNR gap between joint SWD and HD DF relaying in [7] is given as follows:

Lemma 5. *For the same outage at high SNR, the SNR gap Γ_1 (in dB) between FD DF relaying with joint SWD and HD scheme [7] is given as follows:*

$$\begin{aligned}\Gamma_4 &= SNR_{JSWD} - SNR_{HD},\\ &= 5\log(1+2^{2R}) - 5\log(1+0.25(2^R+1)^2),\end{aligned} \tag{32}$$

Proof. Obtained by comparing the high SNR outage of joint SWD in Lemma 5 with that of HD DF scheme in [[6], Theorem 3], which can be optimized to become as follows:

$$\mathbb{P}_{o,\infty}^{HD} = \frac{(2^R-1)^2}{2\mu_{ds}\mu_{rs}}P^{-2} + \frac{(2^{2R}-1)^2}{8\mu_{ds}\mu_{rs}}P^{-2} \tag{33}$$

Then, by setting $10\log(\mathbb{P}_{o,\infty}^{JSWD}) = 10\log(\mathbb{P}_{o,\infty}^{HD})$, we obtain the SNR gap in (32). □

Remark 7. According to (32), $\Gamma_4 > 0$ for any $R > 0$. Hence, at high SNR, HD DF outperforms FD DF with SWD. More discussions are given in Section VII-C. Moreover, Γ_4 depends on the target rate (R) only but not on channel gains.

Remark 8. Similar to remark 6, the SNR gap (Γ_5) between FD DF with BD and HD DF is the sum of Γ_1 and Γ_4.

Remark 9. From the delay, outage, and coding gain analyses in Sections IV, and VI-B, respectively, there is a clear tradeoff between delay and outage performance as BD has longer delay than SWD but better outage performance.

VII. Numerical Results

We now provide numerical results for decoding delay and outage using our derived expressions. In our Monte Carlo simulations, $\mathcal{S}$ and $\mathcal{R}$ have identical transmit powers ($P_s = P_r = P$) and all links experience Rayleigh fading and the average channel gain for each link from node j to i is given as $\mu_{ij} = \frac{1}{dij^{\alpha}}$ with a pathloss factor $\alpha = 2.4$. The average received SNR in dB at $\mathcal{D}$ for the signal from $\mathcal{S}$ is defined as

$$\text{SNR} = 10\log_{10}\left(P/d_{ds}^{\alpha}\right). \tag{34}$$

To optimize (minimize) the outage, the simulations vary the power parameters (ρ_1, ρ_2) for joint and sequential SWD and the binning rate (R_b) for sequential SWD.

A. Average Decoding Delay

Fig. 3 shows the decoding delays of BD and SWD versus B for several node distances. Analytical results and Monte Carlo simulations (10^6 realizations) match perfectly. The delay for SWD is always one while for BD, it increases as B increases and d_{rs} decreases. This is because for any block k with $\mathcal{S}-\mathcal{R}$ link stronger than $\mathcal{S}-\mathcal{D}$, the delay for BD is $B-k$. However, the delay for SWD is $n \in \{1,2,,B-k\}$ and the probability of decoding in block m ($m = k+n$) decreases as n increases.

Figures 4 and 5 study the impact of $\mathcal{R}$ location by showing

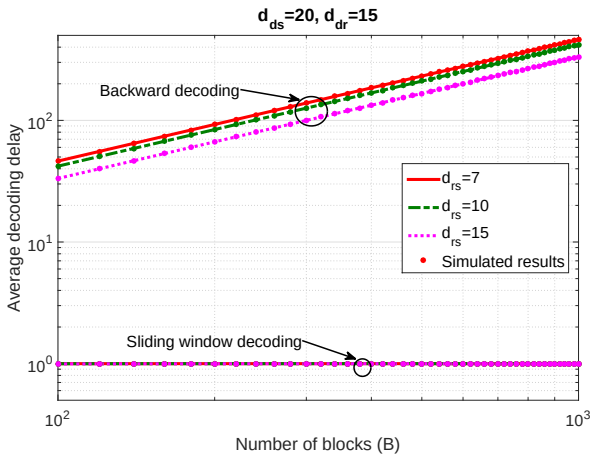

Fig. 3. Decoding delay of BD and SWD versus the number of block (B) with $d_{ds} = 20$, $d_{dr} = 15$ and different d_{rs}.

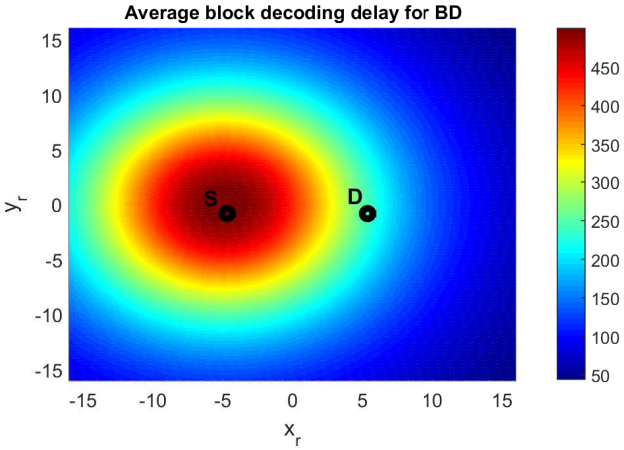

Fig. 4. Decoding delay of FD DF relaying with BD for any $\mathcal{R}$ location in $2D$ plan where $B = 1000$.

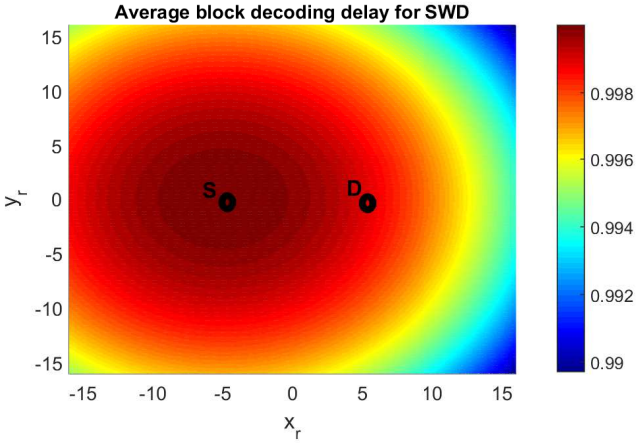

Fig. 5. Decoding delay of FD DF relaying with SWD for any $\mathcal{R}$ location in $2D$ plan where $B = 1000$.

the average decoding delay as a function of the coordinates of $\mathcal{R}$, (x_r, y_r). The locations of $\mathcal{S}$ and $\mathcal{D}$ are fixed at $(-5, 0)$ and $(5, 0)$. These inter-node distances are valid for 5G small cells of 200 m radii [2]. The channel gains (μ_{rs} and μ_{ds}) vary for each $\mathcal{R}$ location which affect the delay considering (12) and (15) formulas. Similar to Fig. 3, BD is highly sensitive to $\mathcal{R}$ location and B (varying between 50 and 480), whereas that of SWD is virtually static (e.g., between 0.99 and 1).

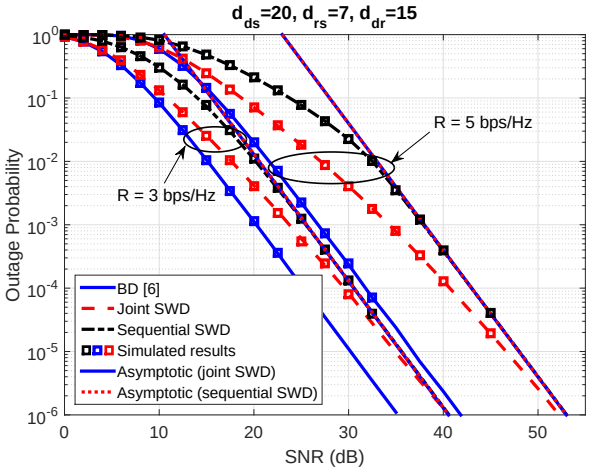

Fig. 6. Outage probabilities of FD DF relaying with BD, joint and sequential SWD at different target rates R.

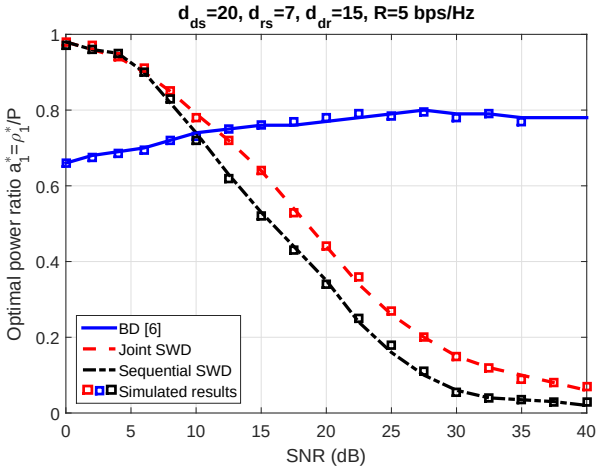

Fig. 7. Optimal power allocation portion $a_1^* = \rho_1^*/P$ to minimize outages of FD DF relaying with BD, joint and sequential SWD.

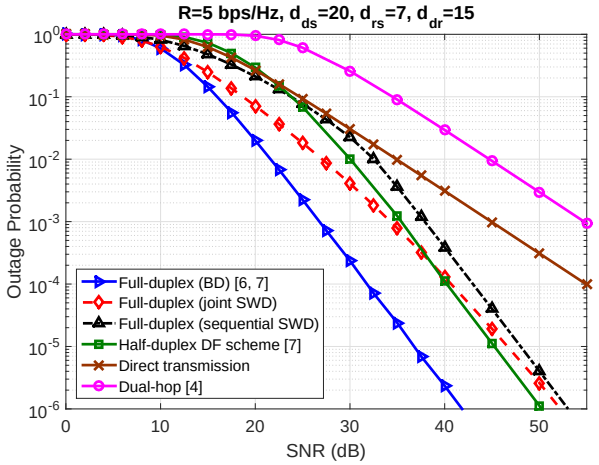

Fig. 8. Outage probabilities of FD DF relaying with BD and SWD (SWD), HD DF relaying [7], dual-hop [4] and direct transmissions at $R = 5$ bps/Hz.

As shown in Theorems 1 and 2, the delay of SWD is less than 1 while it can reach $B/2$ in BD. Besides, in both schemes, the delay increases as $\mathcal{R}$ gets closer to $\mathcal{S}$ since the DF mode occurs more often than DT mode as the probability of having $\mathcal{S}-\mathcal{R}$ link stronger than $\mathcal{S}-\mathcal{D}$ link increases (Section IV).

B. Outage Behavior and Diversity Order

Fig. 6 shows the outage probabilities versus SNR for BD [42], joint and sequential SWD of the FD DF relaying scheme along with the node distances. Monte Carlo simulations (2×10^6 realizations) match perfectly with our analytical results. All decoding techniques achieve a diversity order of two. However, BD has the best outage performance while sequential decoding has the worst. For delay-sensitive applications, joint SWD appears best due to its shorter decoding delay than BD and better outage performance than sequential decoding.

The asymptotic outage curves in Theorem 5 coincide with exact curves of SWD at high SNR. For joint and sequential SWD, the asymptotic curves are almost identical which is expected from Proposition 1 as the coding gain gap $\Gamma_2 \approx 0$ for $R = 3$ and 5 bps/Hz. In contrast, between BD and joint SWD, the coding gain gap Γ_1 at outage$= 10^{-6}$ is 5.54 (11.17) dB for $R = 3$ (5) bps/Hz. Lemma 3 leads to quite close values where $\Gamma_1 = 5.47$ (11.46) dB for $R = 3$ (5) bps/Hz.

Fig. 7 illustrates the optimal power ratio $a_1^* = \rho_1^*/P$ from $\mathcal{S}$ to its new information versus SNR with different decoding techniques. For joint and sequential SWD, a_1^* decreases as SNR increases. These results match the conclusions from Theorem 5 about the required constraint on $a_1 < 2^{-R}$ to achieve a full diversity order of two. For BD, the optimal a_1^* is less sensitive to SNR (slightly increases with SNR). This implies that at high SNR, $\mathcal{R}$ experiences higher outages than $\mathcal{D}$. Hence, considering the rate constraints C_1 and C_2 in (6), $\mathcal{S}$ allocates more power to the new information in each transmission block in order to reduce the outage at $\mathcal{R}$.

C. Comparison with Existing Schemes

Fig. 8 compares the outage probabilities of DT, dual-hop transmission [4], full and HD DF relaying schemes. For the HD scheme, we consider the coherent full DF relaying and joint decoding at $\mathcal{D}$ since [7] shows that it outperforms all other existing HD schemes [5], [8], [9][2]. While FD DF relaying with BD outperforms HD DF relaying, FD DF relaying with SWD underperforms HD DF relaying [7] at high SNR, which is expected from Lemma 5. According to this Lemma, the coding gain gap Γ_4 is -2.87 dB which matches the gap $\Gamma_4 = -2.93$ dB at outage$= 10^{-6}$ in Fig. 8.

In HD [7], each block is divided into 2 phases: broadcast and coherent relaying phases, which reduces the achievable rate and the outage performance. However, in SWD, $\mathcal{D}$ treats the new information of block m as noise which creates the interference shown in (7) and (9). Therefore, results imply that at low SNR, FD with SWD outperforms HD DF because of the rate loss that stems from dividing each transmission block into two phases. However, at high SNR, HD outperforms FD since the interference in SWD becomes significant. While $\mathcal{S}$ can reduce this interference by allocating 2^{-R} or less portion of its power to the new information, this power allocation increases the outage at $\mathcal{R}$ as shown in Theorem 5.

Fig. 9 considers the channel settings in Fig. 8 and illustrates the threshold SNR below which FD DF scheme with joint and/or sequential SWD outperforms HD DF scheme in [7] for

[2]Partial DF relaying outperforms full DF relaying in HD transmission at low SNR [7]. However, it has more parameters to optimize like rate and power allocation for public and private message parts [7].

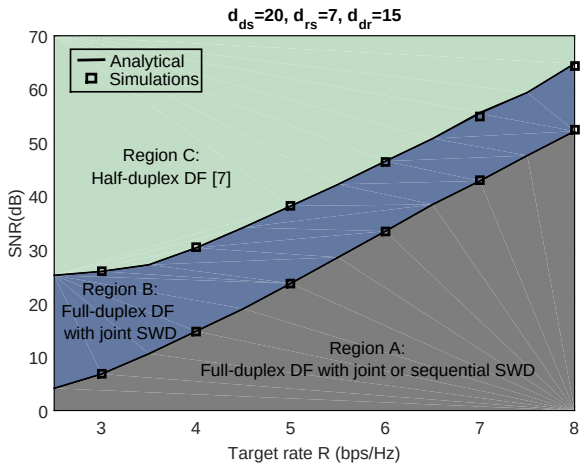

Fig. 9. Threshold SNR below which joint and/or sequential SWD outperforms HD scheme in [7].

different target rates. In region A, both joint and sequential SWD outperform the HD scheme in [7]; in region B, only joint SWD outperforms HD scheme while in region C, neither joint or sequential SWD outperforms the HD scheme. Hence, HD scheme is preferred at high SNR and high target rate.

It is also observed that for $R > 3.5$ bps/Hz, the threshold SNR is almost a linear function of the target rate R, with a slope of 9.3 (8.3) for sequential (joint) SWD. This simple relation can be appealing to the practical designers since by knowing only the SNR, they can decide between FD joint or sequential SWD or HD DF relaying for the best performance.

Figures 8 and 9 imply that depending on the required rate, outage and latency, switching among HD and FD relaying with BD or SWD is an optimal strategy. 5G networks envisage such switching among multiple radio access technologies [2], [11].

VIII. Conclusion

Full-duplex decode-forward relaying is an extremely important technology enabler for 5G wireless. We have derived the decoding delay and outage for joint and sequential sliding window decoding techniques. Both large scale pathloss and small-scale Rayleigh fading were considered. Diversity orders, SNR gaps and coding gains were derived in detail. Our analysis and numerical results imply that different schemes are optimal for different applications depending on the throughput, reliability, and delay requirements. However, generally, joint sliding window decoding has the advantages of shorter decoding delay than backward decoding, better outage performance and fewer parameters to optimize than sequential decoding.

Appendix A: Proof of Theorems 1 and 2

The average decoding delay for BD and SWD is derived.

A.1: Proof of Theorem 1

First, we sum the decoding delay at each block k (T_k^{BD}) in (11) over all $k \in \{1, 2, ..., B-1\}$ and divide over $B-1$ to obtain $\overline{T}^{BD}$ as follows:

$$\begin{aligned}\overline{T}^{BD} &= \frac{\sum_{k=1}^{B-1} \frac{\mu_{rs}}{\mu_{rs}+\mu_{ds}}(B-k)}{B-1}, \\ &= \frac{\mu_{rs}}{\mu_{rs}+\mu_{ds}} \frac{\sum_{k=1}^{B-1} B - \sum_{k=1}^{B-1} k}{B-1}, \end{aligned} \tag{35}$$

Then, applying he summation identity $\sum_{k=1}^{n} k = 0.5n(n+1)$ to $\sum_{k=1}^{B-1} k$, we obtain $\overline{T}^{BD}$ in (12).

A.2: Proof of Theorem 2

First, let $\upsilon_1 = \frac{\mu_{rs}}{\mu_{rs}+\mu_{ds}}$ and $\upsilon_2 = 1 - \upsilon_1 = \frac{\mu_{ds}}{\mu_{rs}+\mu_{ds}}$. Then, we simplify (T_k^{SWD}) in (14) as follows:

$$T_k^{SWD} = \upsilon_1 \left[\frac{\mu_{rs}}{\mu_{ds}} \sum_{i=1}^{B-(k+1)} i\upsilon_2^i + (B-k)\upsilon_2^{B-k}\upsilon_2^{-1} \right], \tag{36}$$

Now, we simplify the first term as follows:

$$\begin{aligned} &\frac{\mu_{rs}}{\mu_{ds}} \sum_{i=1}^{B-(k+1)} i\upsilon_2^i \\ &\overset{(a)}{=} \frac{\mu_{rs}}{\mu_{ds}} \upsilon_1^{-2} \Big(\upsilon_2 - (B-k)\upsilon_2^{B-k} + (B-(k+1))\upsilon_2^{B-k+1} \Big), \\ &= \frac{\mu_{rs}}{\mu_{ds}} \upsilon_1^{-2} \Big(\upsilon_2 - (B-k)\upsilon_2^{B-k}\upsilon_1 - \upsilon_2^{B-k+1} \Big), \\ &= \upsilon_1^{-1} \left(1 + \upsilon_2^{B-k}\right) - (B-k)\upsilon_2^{-1}\upsilon_2^{B-k}, \end{aligned} \tag{37}$$

where (a) is obtained from the identity $\sum_{i=0}^{n} ix^i = \frac{x-(n+1)x^{n+1}+nx^{n+2}}{(x-1)^2}$. By substituting (37) into (36), we obtain

$$T_k^{SWD} = 1 + \upsilon_2^{B-k}. \tag{38}$$

Second, we sum the decoding delay at each block k (T_k^{SWD}) in (38) over all $k \in \{1, 2, ..., B-1\}$ and divide over $B-1$ to obtain $\overline{T}^{SWD}$ as follows:

$$\overline{T}^{SWD} = \frac{\sum_{k=1}^{B-1} 1 + \upsilon_2^{B-k}}{B-1} = \frac{B-1+\upsilon_2^B \sum_{k=1}^{B-1} \upsilon_1^{-k}}{B-1}. \tag{39}$$

Last, by applying he summation identity $\sum_{k=1}^{n} x^k = \frac{x(x^n-1)}{x-1}$ to (39), we obtain $\overline{T}^{SWD}$ in (12).

Appendix B: Proof of Lemma 1

Let $\gamma_1 = g_{ds,k}$, $\gamma_2 = g_{dr,k}$ and $\gamma_3 = g_{rs,k}$ be the channel amplitudes in block i while $\beta_1 = g_{ds,m}$ and $\beta_2 = g_{dr,m}$ be the channel amplitudes in block m. The Rayleigh density for any γ_l, $l \in \{1, 2, 3\}$ or β_l for $l \in \{1, 2\}$ may be given as follows:

$$\mathsf{P}[x_l] = (2x_l/\mu_l) e^{-\frac{x_l^2}{\mu_l}}, \quad 0 \le x < \infty. \tag{40}$$

We may now express outage at $\mathcal{D}$ $(\mathbb{P}_d^{JSWD})$ in (16) as follows:

$$\begin{aligned} \mathbb{P}_d^{JSW} &= \mathsf{P}\big[R > C_3,\ R \le C_1,\ g_{rs,k} > g_{ds,k}\big] &\text{(41a)} \\ &= \mathsf{P}\big[R > C_3,\ \gamma_3 > \eta_2, \gamma_1 \le \gamma_3\big], \\ &= \mathsf{P}\big[\eta_1 < \gamma_1 \le \eta_2,\ \gamma_3 > \eta_2,\ \beta_1 \le \zeta_2,\ \beta_2 \le \zeta_1\big], \\ &= \int_{\eta_1}^{\eta_1} \int_{\eta_2}^{\infty} \int_{0}^{\zeta_2} \int_{0}^{\zeta_1} f_0(\gamma_1, \gamma_3, \beta_1, \beta_2) d\gamma_1 d\gamma_3 d\beta_1 d\beta_2 &\text{(41b)} \end{aligned}$$

where η_1, η_2, ζ_1, and ζ_2 are given in (18) while

$$f_0(\gamma_1, \gamma_3, \beta_1, \beta_2) = \frac{16\gamma_1\gamma_3\beta_1\beta_2}{\mu_{ds}^2\mu_{rs}\mu_{dr}} e^{-\left(\frac{\gamma_1^2}{\mu_{ds}} + \frac{\gamma_3^2}{\mu_{rs}} + \frac{\beta_1^2}{\mu_{ds}} + \frac{\beta_2^2}{\mu_{dr}}\right)} \tag{42}$$

After integrating (41b), we obtain (17) in Lemma 1.

The lower bound on γ_3 is obtained from the second constraint in (41a) as follows:

$$R \le \log\left(1 + \gamma_3^2\rho_1\right), \Leftrightarrow \gamma_3 > \eta_2.$$

From the first constraint in (41a), we obtain the upper bounds on β_1 and β_2 are obtained from (41a) as follows:

$$\left(1+\gamma_1^2\rho_1\right)\left(1+\frac{\left(\beta_1\sqrt{\rho_2}+\beta_2\sqrt{P_r}\right)^2}{1+\beta_1^2\rho_1}\right)\leq 2^R, \Leftrightarrow \beta_2\leq\zeta_1.$$

Similar to β_2, $\beta_1\in[0,\infty)$. Hence, ζ_1 should also be non-negative ($\zeta_1>0$) which adds more constraints on γ_1:

$$\zeta_1\geq 0,\ \Leftrightarrow\ f(\beta_1)\leq 0, \tag{43}$$
$$f(\beta_1)=\beta_1^2\left(P_s(1+\gamma_1^2\rho_1)-2^R\rho_1\right)-\left(2^R-(1+\gamma_1^2\rho_1)\right)$$

Now, let $a = P_s(1+\gamma_1^2\rho_1)-2^R\rho_1$ and $b=-\left(2^R-(1+\gamma_1^2\rho_1)\right)$. Then, it is easy to show that $a>0$ if $\gamma_1>\eta_1$ and $b<0$ if $\gamma_1<\eta_2$. After that, formula (43) is non-negative in the following cases:

- Case 1 ($a<0$ and $b>0$): this case happens when $\gamma_1>\eta_2$ and $\gamma_1<\eta_1$. However, this case cannot occur since $P_s>\rho_1$. More specifically, if $\gamma_1>\eta_2$, then $\gamma_1>\eta_1$ for sure.
- Case 2 ($a<0$ and $b<0$): this case happens when $\gamma_1<\eta_2$ and $\gamma_1<\eta_1$. In this case $f(\beta_1)\leq 0$ for all $\beta_1\in[0,\infty)$.
- Case 3 ($a>0$ and $b<0$): this case happens when $\gamma_1<\eta_2$ and $\gamma_1>\eta_1$. In this case $f(\beta_1)\leq 0$ for all $\beta_1\in[0,\zeta_2)$.

Now, Since $\gamma_1\in[0,\infty)$, in cases 2 and 3, we obtain the following subcases by checking whether $\frac{2^R}{P_s}-\frac{1}{\rho_1}>0$ or <0:

- If $P_s/\rho_1<2^R$, then $0\leq\beta_1<\infty$ when $0<\gamma_1<\eta_1$ while $0\leq\beta_1<\zeta_2$ when $\eta_1<\gamma_1<\eta_2$.
- If $P_s/\rho_1>2^R$, then $0\leq\beta_1<\zeta_2$ when $0<\gamma_1<\eta_2$.

From the above cases, we obtain formula (17) in Lemma 1.

Appendix C: Proof of Theorem 4

C.1: Outage Probability for the Bin Index

In (19), $\mathbb{P}_{d1}$ is given as follows:

$$\begin{aligned}\mathbb{P}_{d1}&=\mathsf{P}\big[R_b>C_4,\ R\leq C_1,\ g_{rs,k}>g_{ds,k}\big], \qquad (44a)\\ &=\mathsf{P}\big[R_b>C_4\big]\mathsf{P}\big[\gamma_3>\eta_2,\ \gamma_1\leq\gamma_3\big],\\ &=\mathsf{P}\big[\gamma_3>\eta_2,\ \gamma_1\leq\gamma_3\big]\\ &\times\begin{cases}\mathsf{P}\big[\beta_2\leq\zeta_3,\ \beta_1\leq\zeta_4\big], & \text{if } \frac{P_s}{\rho_1}>2^{R_b}\\ \mathsf{P}\big[\beta_2\leq\zeta_3,\ \beta_1\leq\infty\big], & \text{if } \frac{P_s}{\rho_1}\leq 2^{R_b}\end{cases}\\ &=\int_{\eta_2}^{\infty}\int_0^{\gamma_3}\frac{4\gamma_1\gamma_3}{\mu_{ds}\mu_{rs}}e^{-\left(\frac{\gamma_1^2}{\mu_{ds}}+\frac{\gamma_3^2}{\mu_{rs}}\right)}d\gamma_1 d\gamma_3\\ &\times\begin{cases}\int_0^{\zeta_4}\int_0^{\zeta_3}f(\beta_1,\beta_2)d\beta_2 d\beta_1, & \text{if } \frac{P_s}{\rho_1}>2^{R_b}\\ \int_0^{\infty}\int_0^{\zeta_3}f(\beta_1,\beta_2)d\beta_2 d\beta_1, & \text{if } \frac{P_s}{\rho_1}\leq 2^{R_b}\end{cases} \qquad (44b)\end{aligned}$$

where η_2 is given in (18), ζ_3 and ζ_4 are given in (21) and $f(\beta_1,\beta_2)$ is given as

$$f(\beta_1,\beta_2)=\frac{4\beta_1\beta_2}{\mu_{ds}\mu_{dr}}e^{-\left(\frac{\beta_1^2}{\mu_{ds}}+\frac{\beta_2^2}{\mu_{dr}}\right)} \tag{45}$$

After integrating (44b), we obtain (20) in Theorem 4.

The bounds on γ_1 and γ_3 are straightforward. The upper bound on β_2 is obtained from the first constraint in (44a). It is straightforward to show that $R_b>C_4\ \Leftrightarrow\ \beta_2\leq\zeta_3$. We then obtain another bound on β_1 since β_2 is non-negative, i.e., $\zeta_3>0\Leftrightarrow\beta_1\leq\zeta_4$. By checking whether ζ_4^2 is positive or negative, we obtain the following two cases:

- If $P_s/\rho_1>2_b^R$, then $\zeta_4^2>0$, $\beta_1<\zeta_4$ and $\beta_2\leq\zeta_3$.
- If $P_s/\rho_1<2_b^R$, then $\zeta_3>0$, for all $\beta_1\in[0,\infty)$.

From these two cases, we obtain formula (20) in Theorem 4.

C.2: Outage Probability for $\mathcal{S}$ information

In (19), $\mathbb{P}_{d2}$ is given as follows:

$$\begin{aligned}\mathbb{P}_{d2}&=\mathsf{P}\big[R_b\leq C_4,\ R-R_b>C_5,\ R\leq C_1,\ g_{rs,i}>g_{ds,i}\big],\\ &=\mathsf{P}\big[R_b\leq C_4\big]\mathsf{P}\big[\gamma_1\leq\eta_3,\ \gamma_3>\eta_2,\ \gamma_1\leq\gamma_3\big],\\ &=\mathsf{P}\big[R_b\leq C_4\big]\mathsf{P}\big[\gamma_1\leq\eta_3,\ \gamma_3>\eta_2\big],\\ &=\mathsf{P}\big[\gamma_3>\eta_2\big]\mathsf{P}\big[\gamma_1\leq\eta_3\big]\\ &\times\begin{cases}\mathsf{P}\big[\beta_2>\zeta_3,\ \beta_1\leq\zeta_4\big]\\ +\mathsf{P}\big[\beta_2>0,\ \beta_1>\zeta_4\big], & \text{if } \frac{P_s}{\rho_1}>2^{R_b}\\ \mathsf{P}\big[\beta_2>\zeta_3,\ \beta_1>0\big], & \text{if } \frac{P_s}{\rho_1}\leq 2^{R_b}\end{cases}\\ &=e^{-\frac{\eta_2^2}{\mu_{rs}}}\left(1-e^{-\frac{2^{R-R_b}-1}{\rho_1\mu_{ds}}}\right) \qquad (46)\\ &\times\begin{cases}\int_0^{\zeta_4}\int_{\zeta_3}^{\infty}f(\beta_1,\beta_2)d\beta_2 d\beta_1+e^{-\frac{\zeta_4^2}{\mu_{ds}}}, & \text{if } \frac{P_s}{\rho_1}>2^{R_b}\\ \int_0^{\infty}\int_{\zeta_3}^{\infty}f(\beta_1,\beta_2)d\beta_2 d\beta_1, & \text{if } \frac{P_s}{\rho_1}\leq 2^{R_b}\end{cases}\end{aligned}$$

where η_3, ζ_3, and ζ_4 are given in (21) and $f(\beta_1,\beta_2)$ is given in (45). After integrating (46), we obtain (20) in Theorem 4.

The analysis for $\mathbb{P}_{d2}$ is quite similar to that for $\mathbb{P}_{d1}$ except adding a new constraint $R-R_b>C_5$ and inverting the constraint $R_b\leq C_4$. From $R-R_b>C_5$, we get another bound on γ_1 which is $\gamma_1\leq\eta_3$. We further get the following two cases from the constraint $R_b\leq C_4$:

- If $P_s/\rho_1>2_b^R$, then $\zeta_4^2>0$. Hence, we have $\beta_2>\zeta_3$ for $0<\beta_1<\zeta_4$ since $\zeta_3>0$ during this interval of β_1. However, we have $\beta_2>0$ for $\beta_1>\zeta_4$ since $\zeta_3<0$ during this interval of β_1.
- If $P_s/\rho_1<2_b^R$, then $\zeta_3>0$ for all $\beta_1\in[0,\infty)$.

From these two cases, we obtain (20) in Theorem 4.

Appendix D: Derivation of $\mathbb{P}_{d,\infty}^{JSWD}$

Starting from the outage expressions in Lemma 1, we can show that at high SNR, ζ_1 and ζ_2 in (18) are given as follows:

$$\begin{aligned}\zeta_{1,\infty}&=\frac{\beta_1}{P}\left(\sqrt{2^R/\gamma_1^2-\rho_1}-\sqrt{\rho_2}\right),\\ &=\beta_1\left(\sqrt{2^R/(\gamma_1^2P)-a_1}-\sqrt{a_2}\right),\\ \zeta_{2,\infty}&=\sqrt{(2^R-1-\gamma_1^2\rho_1)/(P+P\gamma_1^2\rho_1-2^R\rho_1)},\\ &=\sqrt{\frac{\frac{2^R-1}{\gamma_1^2P}-a_1}{a_1P\left(\frac{1}{\gamma_1^2P}\left(\frac{1}{a_1}-2^R\right)+1\right)}} \qquad (47)\end{aligned}$$

Then, considering (17), we analyze the integrals when $P_s/\rho_1>2^R$ and $P_s/\rho_1>2^R$.

D.1: When $P_s/\rho_1>2^R$

First, considering $\zeta_{1,\infty}$ in (47), we approximate $f(\gamma_1,\beta_1,\zeta_{1,\infty})$ in (18) as follows:

$$\begin{aligned}f(\gamma_1,\beta_1,\zeta_{1,\infty})&=\frac{4\gamma_1\beta_1}{\mu_{ds}^2}e^{-\frac{\gamma_1^2+\beta_1^2}{\mu_{ds}}}\left(1-e^{-\frac{\zeta_{1,\infty}^2}{\mu_{dr}}}\right)\\ &\overset{(a)}{\approx}\frac{4\gamma_1\beta_1}{\mu_{ds}^2}\left(1-\frac{\gamma_1^2+\beta_1^2}{\mu_{ds}}\right)\frac{\zeta_{1,\infty}^2}{\mu_{dr}},\\ &\overset{(b)}{\approx}\frac{4\gamma_1\beta_1}{\mu_{ds}^2}\frac{\beta_1^2}{\mu_{dr}}\left(\sqrt{2^R/(\gamma_1^2P)-a_1}-\sqrt{a_2}\right)^2, \qquad (48)\end{aligned}$$

where (a) is obtained by the first-order Taylor series expansion $e^{-x} = 1 - x$ and (b) is obtained by smallest order of γ_1 and β_1 since their integral limits are proportional to $1/P$.

Next, we approximate the first integration in (17) as follows:

$$\mathbb{P}_{d,\infty}^{JSW} \approx \int_0^{\eta_{1,\infty}} \int_0^{\zeta_{2,\infty}} \frac{4\gamma_1\beta_1^3}{\mu_{ds}^2\mu_{dr}} \left(\sqrt{2^R/(\gamma_1^2 P) - a_1} - \sqrt{a_2}\right)^2 \partial\beta_1 \partial\gamma_1, \stackrel{(a)}{=} \int_0^{\eta_{1,\infty}} \frac{\gamma_1\zeta_{2,\infty}^4}{\mu_{ds}^2\mu_{dr}} \left(\sqrt{2^R/(\gamma_1^2 P) - a_1} - \sqrt{a_2}\right)^2 \partial\gamma_1, \quad (49)$$

where (a) is obtained by evaluating the integral over β_1 and $\zeta_{2,\infty}$ is given in (47). Then, by substituting $x = \frac{1}{\gamma_1^2 P}$, we obtain the first integral in Lemma 5 for $P/\rho_1 > 2^R$.

D.2: When $P_s/\rho_1 < 2^R$

At high SNR, P_d^{JSW} can be expressed as follows:

$$\begin{aligned} P_{d,\infty}^{JSW} &= e^{-\frac{\eta_2^2}{\mu_{rs}}} \int_0^{\sqrt{2^R/P_s}} \int_0^{\infty} f(\gamma_1, \beta_1, \zeta_{1,\infty}) d\beta_1 d\gamma_1, \\ &\stackrel{a}{=} e^{-\frac{\eta_2^2}{\mu_{rs}}} \left(1 - e^{-\frac{2^R}{\mu_{ds} P_s}}\right) - e^{-\frac{\eta_2^2}{\mu_{rs}}} \\ &\times \int_0^{\sqrt{2^R/P_s}} \frac{\frac{2\gamma_1}{\mu_{ds}} e^{\frac{-\gamma_1^2}{\mu_{ds}}} \mu_{dr}}{\mu_{dr} + \mu_{ds}\left(\sqrt{\frac{2^R}{\gamma_1^2 P_r} - a_1} - \sqrt{a_2}\right)^2} d\gamma_1, \\ &\stackrel{b}{\approx} \left(1 - \frac{\eta_2^2}{\mu_{rs}}\right) \frac{2^R}{\mu_{ds} P_s} - \left(1 - \frac{\eta_2^2}{\mu_{rs}}\right) \\ &\times \int_0^{\sqrt{2^R/P_s}} \frac{\frac{2\gamma_1}{\mu_{ds}}\left(1 - \frac{\gamma_1^2}{\mu_{ds}}\right) \mu_{dr}}{\mu_{dr} + \mu_{ds}\left(\sqrt{\frac{2^R}{\gamma_1^2 P_r} - a_1} - \sqrt{a_2}\right)^2} d\gamma_1, \\ &\stackrel{c}{\approx} \frac{2^R}{\mu_{ds} P_s} - \int_0^{\sqrt{2^R/P_s}} \frac{\frac{2\gamma_1}{\mu_{ds}} \mu_{dr}}{\mu_{dr} + \mu_{ds}\left(\sqrt{\frac{2^R}{\gamma_1^2 P_r} - a_1} - \sqrt{a_2}\right)^2} d\gamma_1 \\ &\stackrel{d}{=} \frac{2^R}{\mu_{ds} P_s}(1 - K_2), \end{aligned} \quad (50)$$

where K_2 is given in (26). In (50), (a) is obtained by evaluating the integral over β_1; (b) is obtained from the first order Taylor series expansion $e^{-x} \approx 1 - x$; (c) is obtained by considering the factors that lead to the lowest order of P_s as the higher orders will be redundant at high SNR; and (d) is obtained by using integration by substitution where we set $x = \frac{2^R}{\gamma_1^2 P_s} - a_1$ and perform some mathematical manipulations.

Appendix E: Derivation of $\mathbb{P}_{d,\infty}^{SSWD}$

Starting from the outage expressions in Theorem 4, it is easy to show that at high SNR, ζ_3 in (21) is given as follows:

$$\zeta_{3,\infty} = \beta_1 \left(\sqrt{(2^{R_b} - 1)a_1} - \sqrt{a_2}\right). \quad (51)$$

Then, $f_1(\beta_1, \zeta_{3,\infty})$ in (21) can be expressed as follows:

$$\begin{aligned} f_1(\beta_1, \zeta_{3,\infty}) &= \frac{2\beta_1}{\mu_{ds}} e^{-\frac{\beta_1^2}{\mu_{ds}}} \left(1 - e^{-\frac{\beta_1^2\left(\sqrt{(2^{R_b}-1)a_1} - \sqrt{a_2}\right)^2}{\mu_{dr}}}\right), \\ &\stackrel{(a)}{\approx} \frac{2\beta_1^3}{\mu_{ds}} \frac{\left(\sqrt{(2^{R_b} - 1)a_1} - \sqrt{a_2}\right)^2}{\mu_{dr}}. \end{aligned} \quad (52)$$

where (a) is obtained from the first order Taylor series expansion for $e^{-x} = 1 - x$. Similarly, we approximate $f_2(\beta_1, \zeta_{3,\infty})$ in (21) as follows:

$$f_2(\beta_1, \zeta_{3,\infty}) \approx 2\beta_1/\mu_{ds}. \quad (53)$$

Then, we can easily approximate the outages for the bin index and $\mathcal{S}$ information as follows.

E.1: Outage Probability for the Bin Index

Using (51) and (52), we approximate $P_{d1,\infty}^{SSW}$ in (20) as follows:

$$\begin{aligned} P_{d1,\infty}^{SSW} &\approx \left(e^{-\frac{\eta_2}{\mu_{rs}}} - \frac{\mu_{ds}}{\mu_{ds} + \mu_{rs}} e^{-\frac{\eta_2(\mu_{ds} + \mu_{rs})}{\mu_{ds}\mu_{rs}}}\right) \\ &\times \begin{cases} \int_0^{\zeta_4} f_1(\beta_1, \zeta_{3,\infty}) d\beta_1, & \text{if } \frac{P_s}{\rho_1} > 2^{R_b} \\ \int_0^{\infty} f_1(\beta_1, \zeta_{3,\infty}) d\beta_1, & \text{if } \frac{P_s}{\rho_1} \le 2^{R_b} \end{cases} \\ &\stackrel{a}{\approx} \frac{\mu_{rs}}{\mu_{ds} + \mu_{rs}} \times \begin{cases} \int_0^{\zeta_4} f_1(\beta_1, \zeta_{3,\infty}) d\beta_1, & \text{if } \frac{P_s}{\rho_1} > 2^{R_b} \\ \int_0^{\infty} f_1(\beta_1, \zeta_{3,\infty}) d\beta_1, & \text{if } \frac{P_s}{\rho_1} \le 2^{R_b} \end{cases} \end{aligned} \quad (54)$$

where (a) is obtained by using the Taylor series expansion $e^{-x} \approx 1 - x$. Evaluating the integral over β_1 leads to (27a).

E.2: Outage Probability for $\mathcal{S}$ information

Following similar steps to $P_{d1,\infty}^{SSW}$ and Using (51) and (53), we can approximate $P_{d2,\infty}^{SSW}$ as follows:

$$\begin{aligned} P_{d2,\infty}^{SSW} &= e^{-\frac{\eta_2^2}{\mu_{rs}}} \left(1 - e^{-\frac{\eta_3^2}{\mu_{ds}}}\right) \\ &\times \begin{cases} e^{-\frac{\zeta_4^2}{\mu_{ds}}} + \int_0^{\zeta_4} f_2(\beta_1, \zeta_{3,\infty}) d\beta_1, & \text{if } \frac{P_s}{\rho_1} > 2^{R_b} \\ \int_0^{\infty} f_2(\beta_1, \zeta_{3,\infty}) d\beta_1, & \text{if } \frac{P_s}{\rho_1} \le 2^{R_b} \end{cases} \end{aligned} \quad (55)$$

We obtain (27b) by evaluating the integral over β_1 considering the first-order Taylor series expansion $e^{-x} \approx 1 - x$.

References

[1] J. Korhonen, *Introduction to 4G mobile communications*. Artech House, 2014.

[2] Y. Niu, Y. Li, D. Jin, L. Su, and A. V. Vasilakos, "A survey of millimeter wave (mmwave) communications for 5G: opportunities and challenges," *available online: http://arxiv.org/abs/1502.07228.*, Feb. 2015.

[3] Ericsson, "5G radio access: capabilities and technologies," *Ericsson White Paper, Uen 284 23-3204 Rev C, Stockholm, Sweden*, Apr. 2016.

[4] M. O. Hasna and M. S. Alouini, "Optimal power allocation for relayed transmissions over Rayleigh fading channels," in *IEEE VTC*, Apr. 2003.

[5] J. Laneman, D. Tse, and G. Wornell, "Cooperative diversity in wireless networks: Efficient protocols and outage behavior," *IEEE Trans. Inf. Theory*, vol. 50, no. 12, pp. 3062 – 3080, Dec. 2004.

[6] L. Pinals, A. Abu Al Haija, and M. Vu, "Link regime and power savings of decode-forward relaying in fading channels," *IEEE Trans. Commun.*, vol. 64, no. 3, pp. 931–946, Mar. 2016.

[7] A. Abu Al Haija and M. Vu, "Outage analysis for coherent decode-forward relaying over Rayleigh fading channels," *IEEE Trans. Commu.*, vol. 63, no. 4, pp. 1162–1177, Apr. 2015.

[8] R. U. Nabar, H. Bolcskei, and F. W. Kneubuhler, "Fading relay channels: performance limits and space-time signal design," *IEEE J. Sel. Areas Commun.*, vol. 22, no. 6, pp. 1099–1109, Aug. 2004.

[9] M. Yuksel and E. Erkip, "Broadcast strategies for the fading relay channel," in *IEEE Milcom.*, vol. 2, 2004.

[10] M. Mohammadi, H. A. Suraweera, Y. Cao, I. Krikidis, and C. Tellambura, "Full-duplex radio for uplink/downlink wireless access with spatially random nodes," *IEEE Trans. Commun.*, vol. 63, no. 12, pp. 5250–5266, Dec. 2015.

[11] Z. Zhang, K. Long, A. V. Vasilakos, and L. Hanzo, "Full-duplex wireless communications: challenges, solutions and future research directions," *Proceedings of the IEEE*, vol. 104, no. 7, pp. 1369–1409, July 2016.

[12] A. Sabharwal, P. Schniter, D. Guo, D. Bliss, S. Rangarajan, and R. Wichman, "In-band full-duplex wireless: challenges and opportunities," *IEEE J. Sel. Areas Commun.*, vol. 32, no. 9, pp. 1637–1652, Sept. 2014.

[13] Y.-S. Choi and H. Shirani-Mehr, "Simultaneous transmission and reception: algorithm, design and system level performance," *IEEE Trans. Wireless. Commun.*, vol. 12, no. 12, pp. 5992–6010, Dec. 2013.

[14] D. Bharadia, E. Mcmilin, and S. Katti, "Full duplex radios," *ACM, SIGCOMM*, vol. 43, no. 4, p. 375386, Aug. 2013.

[15] K. Alexandris, A. Balatsoukas-Stimming, and A. Burg, "Measurement-based characterization of residual self-interference on a full-duplex MIMO testbed," in *IEEE SAM Signal Processing Workshop*, June 2014.

[16] A. Altieri, L. Rey Vega, P. Piantanida, and C. G. Galarza, "On the outage probability of the full-duplex interference-limited relay channel," *IEEE J. Sel. Areas Commun.*, vol. 32, no. 9, pp. 1765–1777, Sept. 2014.

[17] T. M. Cover and A. El Gamal, "Capacity theorems for the relay channel," *IEEE Trans. Inf. Theory*, vol. 25, pp. 572–584, Sep. 1979.

[18] R. El Gamal and Y.-H. Kim, *Network Information Theory*, 1st ed. Cambridge University Press, 2011.

[19] L.-L. Xie and P. Kumar, "An achievable rate for the multiple-level relay channel," *IEEE Trans. on Info. Theory*, vol. 51, no. 4, pp. 1348–1358, Apr. 2005.

[20] A. Abu Al Haija and M. Vu, "Outage analysis for half-duplex partial decode-forward relaying over fading channel," in *IEEE GLOBECOM*, Dec. 2014.

[21] M. Maaz, P. Mary, and M. Helard, "Delay outage probability in block fading channel and relay-assisted Hybrid-ARQ network," *IEEE Wireless Commun. Lett.*, vol. 3, no. 2, pp. 129–132, Apr. 2014.

[22] A. S. Avestimehr and D. Tse, "Outage capacity of the fading relay channel in the low-SNR regime," *IEEE Trans. Inf. Theory.*, vol. 53, no. 4, pp. 1401–1415, Apr. 2007.

[23] K. Azarian, H. El Gamal, and P. Schniter, "On the achievable diversity-multiplexing tradeoff in half-duplex channels," *IEEE Trans. Inf. Theory.*, vol. 51, no. 12, pp. 4152–4172, Dec. 2005.

[24] D. Gunduz and E. Erkip, "Opportunistic cooperation by dynamic resource allocation," *IEEE Trans. Wireless. Commun.*, vol. 6, no. 4, pp. 1446–1454, Apr. 2007.

[25] J. S. Wang, Y. H. Kim, I. Song, P. C. Cosman, and L. B. Milstein, "Cooperative relaying of superposition coding with simple feedback for layered source transmission," *IEEE Trans. Commun.*, vol. 61, no. 11, pp. 4448–4461, Nov. 2013.

[26] A. Host-Madsen and J. Zhang, "Capacity bounds and power allocation for wireless relay channels," *IEEE Trans. Inf. Theory.*, vol. 51, no. 6, pp. 2020–2040, Jun. 2005.

[27] A. Abu Al Haija and M. Vu, "Spectral efficiency and outage performance for hybrid D2D-infrastructure uplink cooperation," *IEEE Trans. Wireless Commu.*, vol. 14, no. 3, pp. 1183–1198, Mar. 2015.

[28] C. Hucher, G. Othman, and A. Saadani, "A new incomplete decode-and-forward protocol," in *IEEE WCNC.*, Mar. 2008.

[29] A. Abu Al Haija and M. Vu, "Outage analysis for uplink mobile-to-mobile cooperation," in *Workshop on Device-to-Device Communications, IEEE GLOBECOM*, Dec. 2013, pp. 579–584.

[30] R. Mudumbai, D. Brown, U. Madhow, and H. Poor, "Distributed transmit beamforming: challenges and recent progress," *IEEE Commun. Mag.*, vol. 47, no. 2, pp. 102–110, Feb. 2009.

[31] L. Gerdes, L. Weiland, M. Riemensberger, and W. Utschick, "Optimal partial decode-and-forward rates for stochastically degraded gaussian relay channels," in *IEEE 48th Annual Conference on Information Sciences and Systems (CISS)*, Mar. 2014.

[32] G. Li, J. Chen, Y. Huang, and G. Ren, "Outage performance of multiple-input-multiple-output decode-and-forward relay networks with the Nth-best relay selection scheme in the presence of co-channel interference," *IET Communications*, vol. 8, no. 15, pp. 2762–2773, Oct. 2014.

[33] J. Boyer, D. D. Falconer, and H. Yanikomeroglu, "Multi-hop diversity in wireless relaying channels," *IEEE Trans. Commun.*, vol. 52, no. 10, pp. 1820–1830, Oct. 2004.

[34] B. Maham, A. Behnad, and M. Debbah, "Analysis of outage probability and throughput for half-duplex hybrid-ARQ relay channels," *IEEE Trans. Veh. Technol.*, vol. 61, no. 7, pp. 3061–3070, Sept. 2012.

[35] D. S. Michalopoulos and G. K. Karagiannidis, "Performance analysis of single relay selection in Rayleigh fading," *IEEE Trans. Wireless. Commun.*, vol. 7, no. 10, pp. 3718–3724, Oct. 2008.

[36] M. Benjillali and M. S. Alouini, "Partner cooperation with decode-and-forward: closed-form outage analysis and comparison," *IEEE Trans. Veh. Technol.*, vol. 62, no. 1, pp. 127–139, Jan. 2013.

[37] L. Pinals and M. Vu, "Link state based decode-forward schemes for two-way relaying," in *International Workshop on Emerging Technologies for 5G Wireless Cellular Networks (GLOBECOM),*, Dec. 2014.

[38] A. El Gamal, M. Mohseni, and S. Zahedi, "Bounds on capacity and minimum energy-per-bit for AWGN relay channels," *IEEE Trans. Inf. Theory.*, vol. 52, no. 4, pp. 1545–1561, Apr. 2006.

[39] P. Zhong and M. Vu, "Partial decode-forward coding schemes for the gaussian two-way relay channel," in *IEEE ICC*, June 2012.

[40] Z. Wu and M. Vu, "Partial Decode-Forward Binning for Full-Duplex Causal Cognitive Interference Channels," in *IEEE ICC*, June 2013.

[41] V. Prabhakaran and P. Viswanath, "Interference channels with source cooperation," *IEEE Trans. Inf. Theory*, vol. 57, no. 1, pp. 156–186, Jan. 2011.

[42] A. Abu Al Haija, L. Pinals, and M. Vu, "Outage analysis and power savings for independent and coherent decode-forward relaying," in *IEEE GLOBECOM*, Dec. 2015.

[43] Huawei, "5G: A technology vision," *Huawei Technologies Co., Ltd.*, 2013.

[44] 3GPP, "Lte physical layer framework for performance verification," *TS R1-070674, 3rd Generatin Partnership Project (3GPP), St. Louis, USA*, Feb. 2007.

[45] Z. Wang and G. B. Giannakis, "A simple and general parameterization quantifying performance in fading channels," *IEEE Trans. Comm.*, vol. 51, no. 8, pp. 1389–1398, Aug. 2003.

[46] Y. Dhungana and C. Tellambura, "Uniform approximations for wireless performance in fading channels," *IEEE Trans. Commun.*, vol. 61, no. 11, pp. 4768–4779, Nov. 2013.

Ahmad Abu Al Haija (S'10-M'15) received the B.Sc. and M.Sc. degrees in electrical engineering from Jordan University of Science and Technology (JUST), Irbid, Jordan, and the Ph.D. degree in electrical engineering from McGill University, Montreal, QC, Canada, in 2006, 2009, and 2015, respectively. He is currently a Postdoctoral Fellow with the Electrical and Computer Engineering Department, University of Alberta, Edmonton, AB, Canada. Between February 2013 and August 2014, he was a Visiting Student at Tufts University, Medford, MA, USA. His research interest includes cooperation in multiuser channels, resource allocation for cooperative communication systems, wireless communications and performance analysis and evaluation over fading channels.

Chintha Tellambura (F'11) received the B.Sc. degree (with first-class honor) from the University of Moratuwa, Sri Lanka, in 1986, the M.Sc. degree in Electronics from the University of London, United Kingdom, in 1988, and the Ph.D. degree in Electrical Engineering from the University of Victoria, Canada, in 1993.

He was a Postdoctoral Research Fellow with the University of Victoria (1993-1994) and the University of Bradford (1995-1996). He was with Monash University, Australia, from 1997 to 2002. Presently, he is a Professor with the Department of Electrical and Computer Engineering, University of Alberta. His current research interests include the design, modelling and analysis of cognitive radio networks, heterogeneous cellular networks and multiple-antenna wireless networks.

Prof. Tellambura served as an editor for both IEEE Transactions on Communications and IEEE Transactions on Wireless Communications and was the Area Editor for Wireless Communications Systems and Theory in the IEEE Transactions on Wireless Communications during 2007-2012. Prof. Tellambura and co-authors received the Communication Theory Symposium best paper award in the 2012 IEEE International Conference on Communications, Ottawa, Canada. He is the winner of the prestigious McCalla Professorship and the Killam Annual Professorship from the University of Alberta. Prof. Tellambura has authored or coauthored over 490 journal and conference publications with total citations more than 11,000 and an h-index of 55 (Google Scholar).